The Role of Magnetic Fields in the Stability and Fragmentation of Filamentary Molecular Clouds

SOFIA Tele-talk, November 16, 2022

Pak Shing Li
Department of Astronomy, University of California at Berkeley

Collaborators:

Enrique Lopez-Rodriguez (KIPAC, Stanford University)
Archana Soam (Indian Institute of Astrophysics)
Hamza Ajeddig & Philippe André (Laboratoire d'Astrophysique (AIM))
Jeonghee, Rho (SETI Institute)

Christopher F. McKee & Richard I. Klein (UC Berkeley)

Outline

- Background on observed filamentary molecular clouds
- Inspiration from numerical simulations on the formation of filamentary molecular clouds
- HAWC+ observation of filamentary clouds in OMC-3 and OMC-4 regions in Orion A
- HAWC+ observation of the filamentary cloud in Taurus/B211 region
- Concluding remarks

Filamentary Infrared Dark Clouds (IRDCs)

Vasyunina et al. (2009)

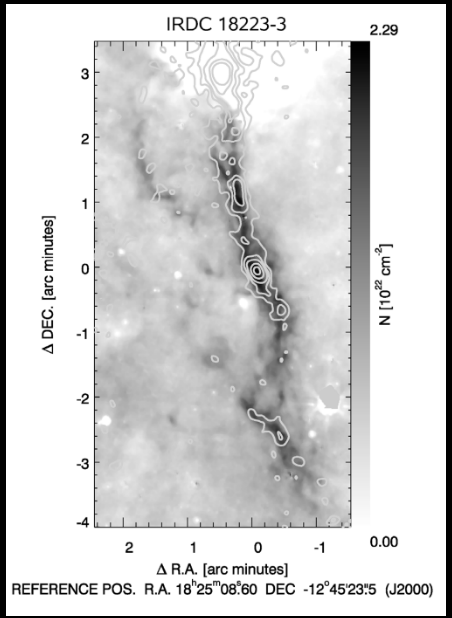

G11.11+0.12 (Bergin & Tafalla 2007)

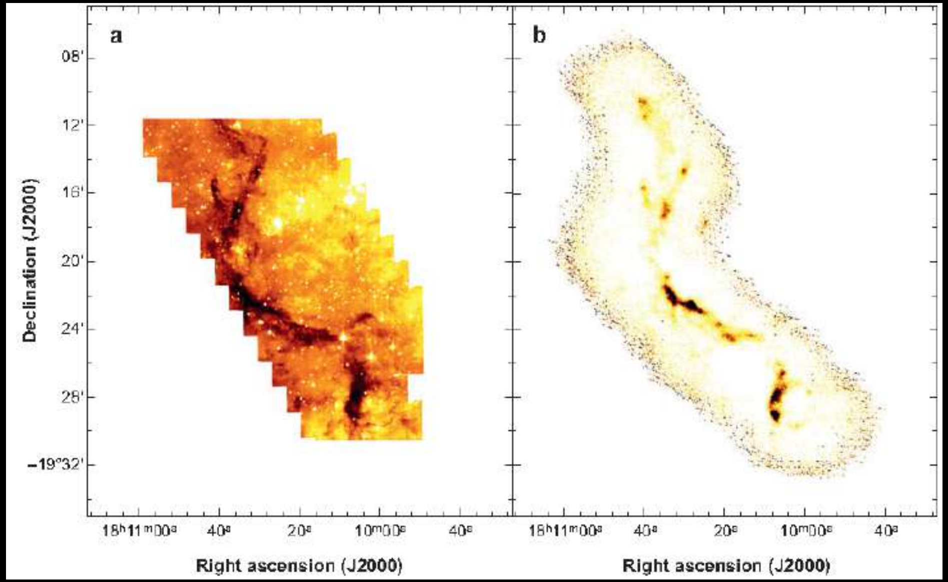

IRDC H 8 μm (Hernandez & Tan 2011)

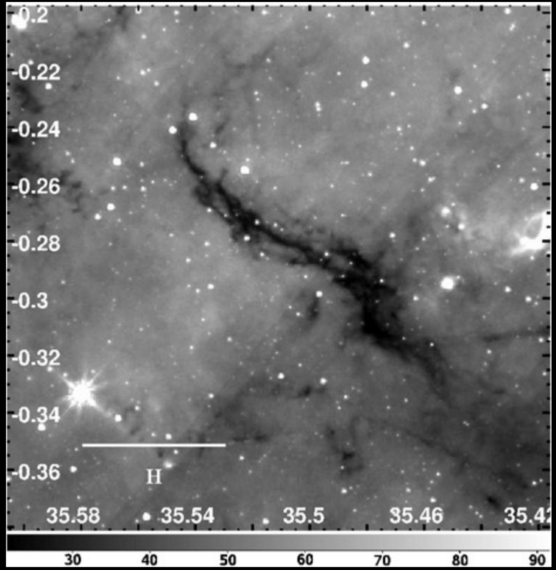

Infrared Dark clouds (IRDCs):

- Opaque against galactic background at mid-IR ~10 μm (opacity 1~4)
- N(H) ≥ 10^{22} cm^{-2}, n(H) ≥ 10^4 cm^{-3}
- Filamentary, a couple to > 10 pc long
- Locations of massive stars and star clusters formation

(e.g., Carey et a. 1998, Egan et al. 1998, Hennebelle et at. 2001, Rathborne el al. 2006, Bergin & Tafalla 2007, Battersby et al. 2010, Peretto & Fuller 2010, Hernandez & Tan 2011, Andre et al. 2015)

Filamentary Structures in Molecular Clouds

Taurus (Panopoulou et al. 2014)

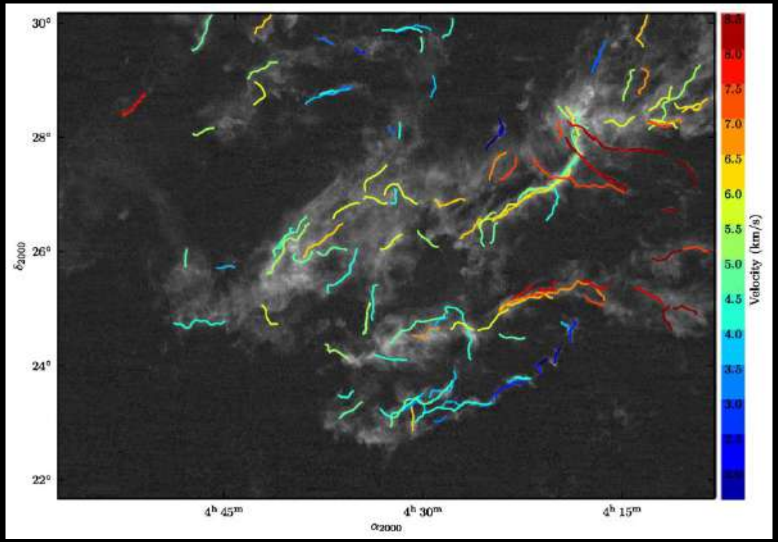

Aquila region (Könyves et al. 2015)

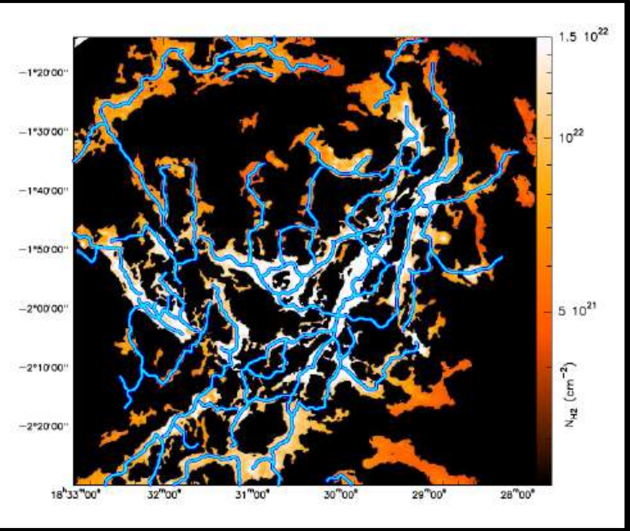

IC5146 (Arzoumanian et al. 2011)

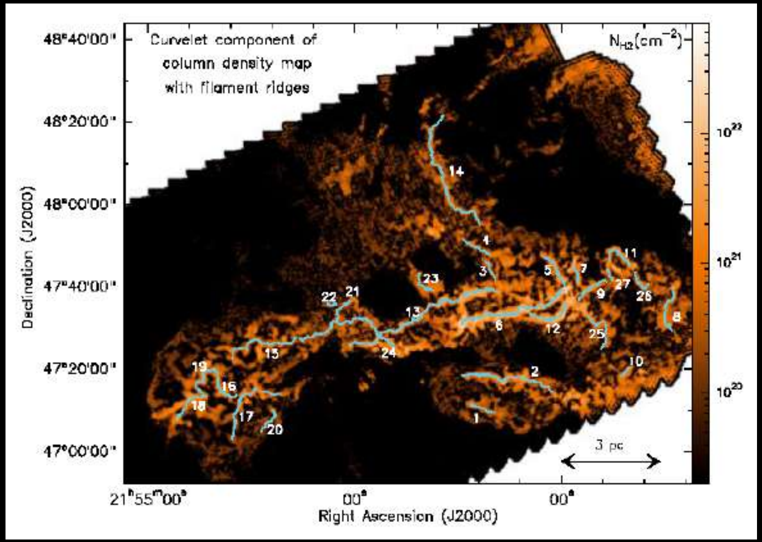

Lupus 1 (Benedettini et al. 2013)

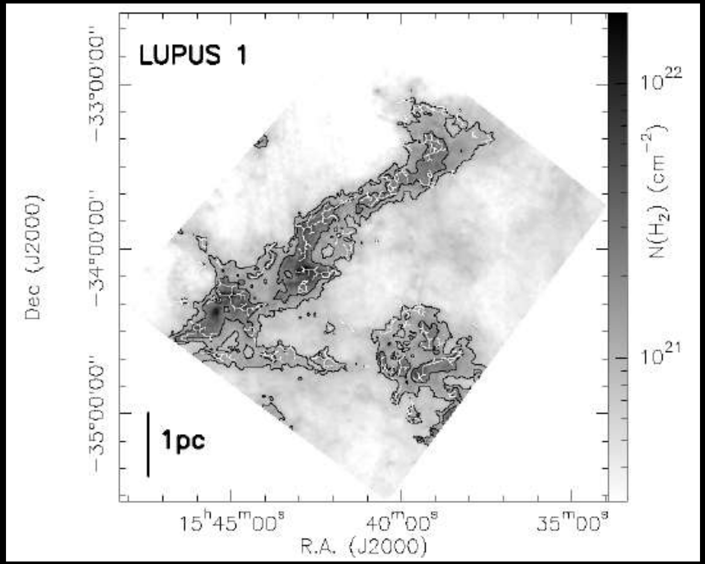

Filamentary Substructures in Filamentary Cloud L1495/B213

Hacar et al. (2013)

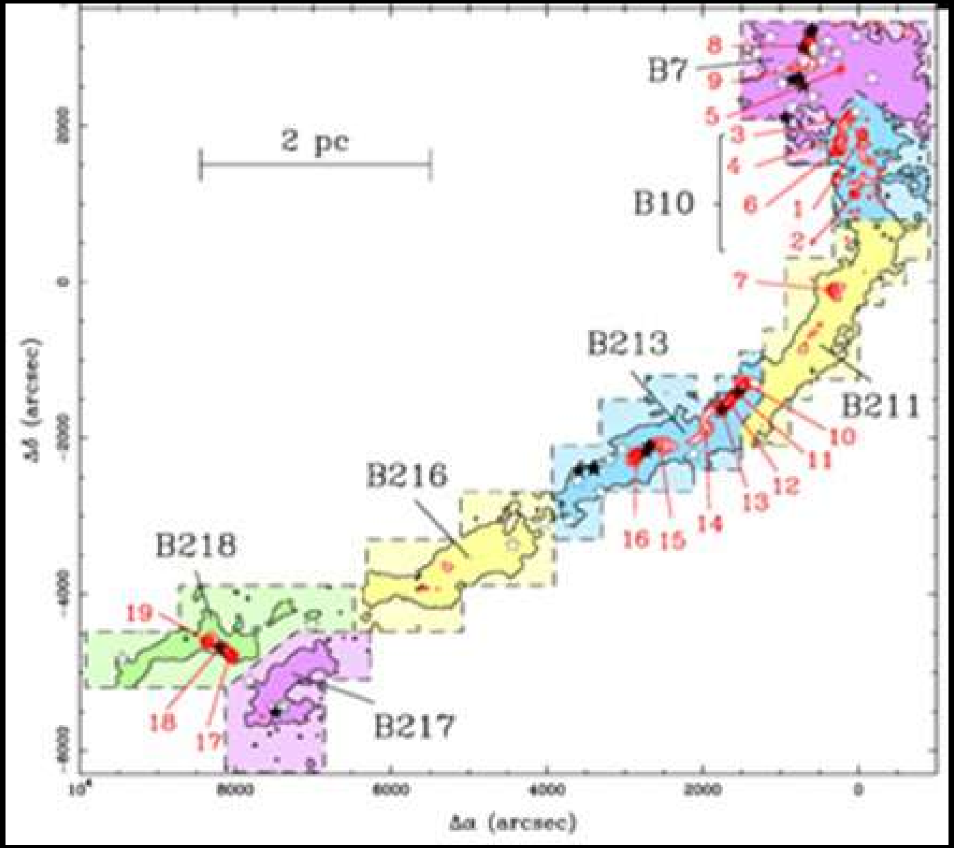

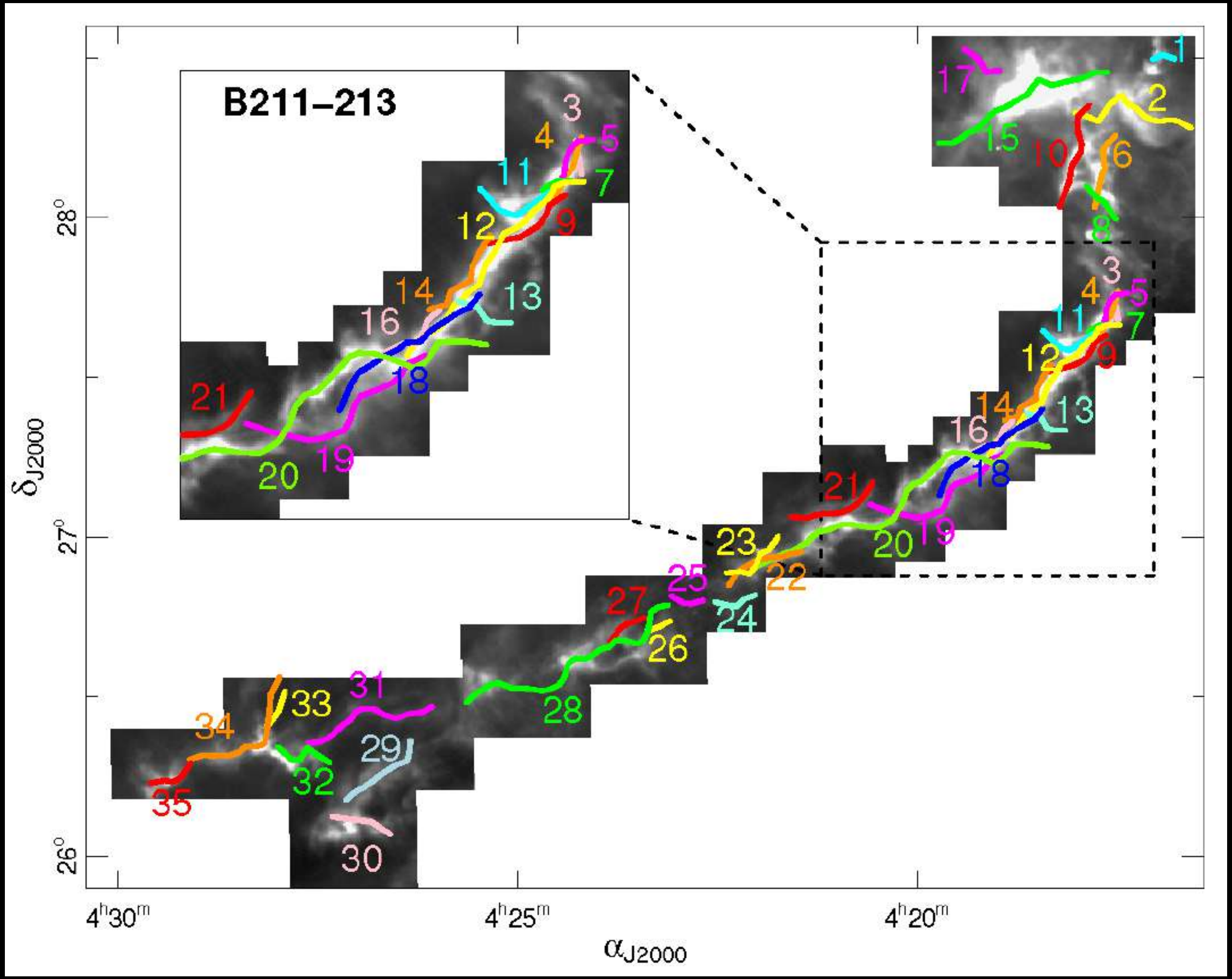

Filaments width ~ 0.1 pc (Arzoumanian et al. 2018)

Cores in Filamentary Sub-structures in Molecular Clouds

L1495/B213 (Hacar et al 2013)

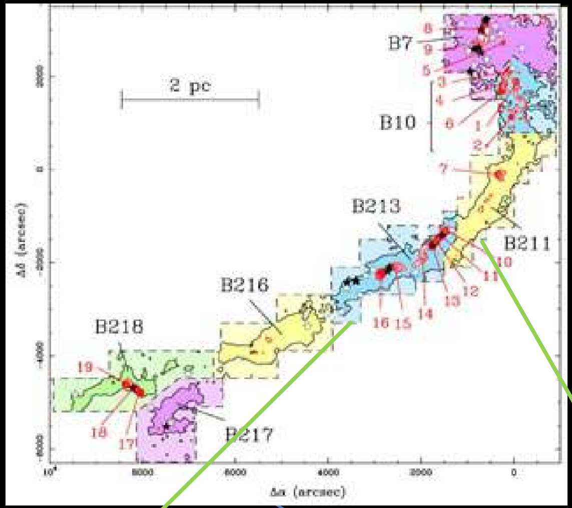

B213 (Tafalla & Hacar 2015)

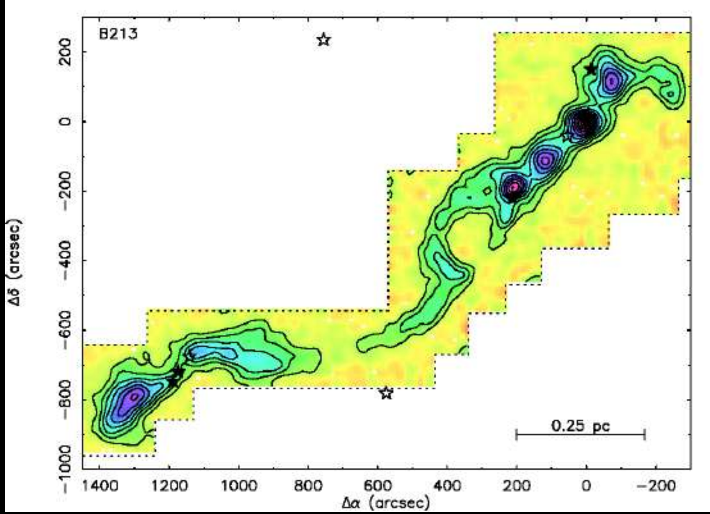

Aquila region (Könyves et al. 2015)

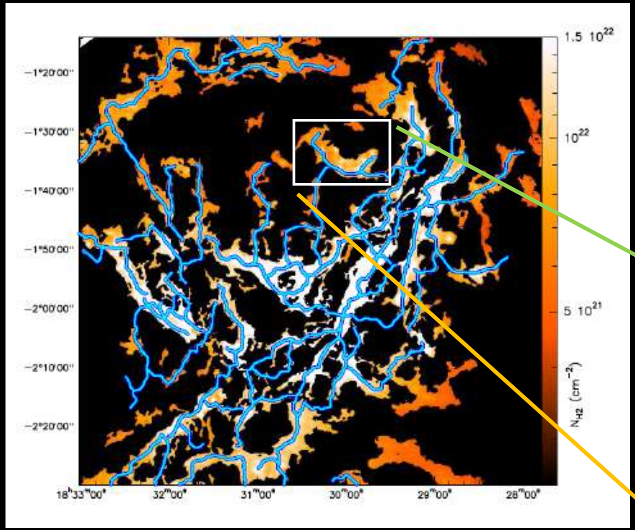

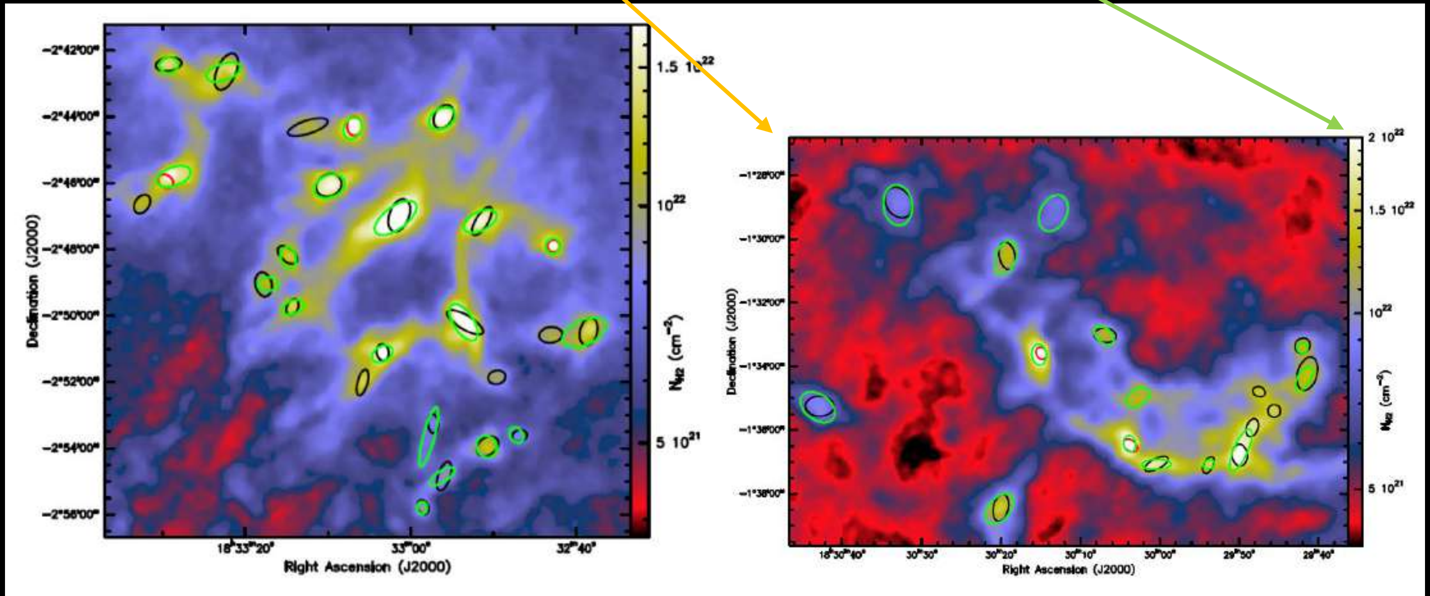

Size hierarchy of gas structures:

GMCs

filamentary clouds

filamentary substructures

cores

Magnetic Field Structures in Filamentary Clouds

Velocity field   Magnetic field

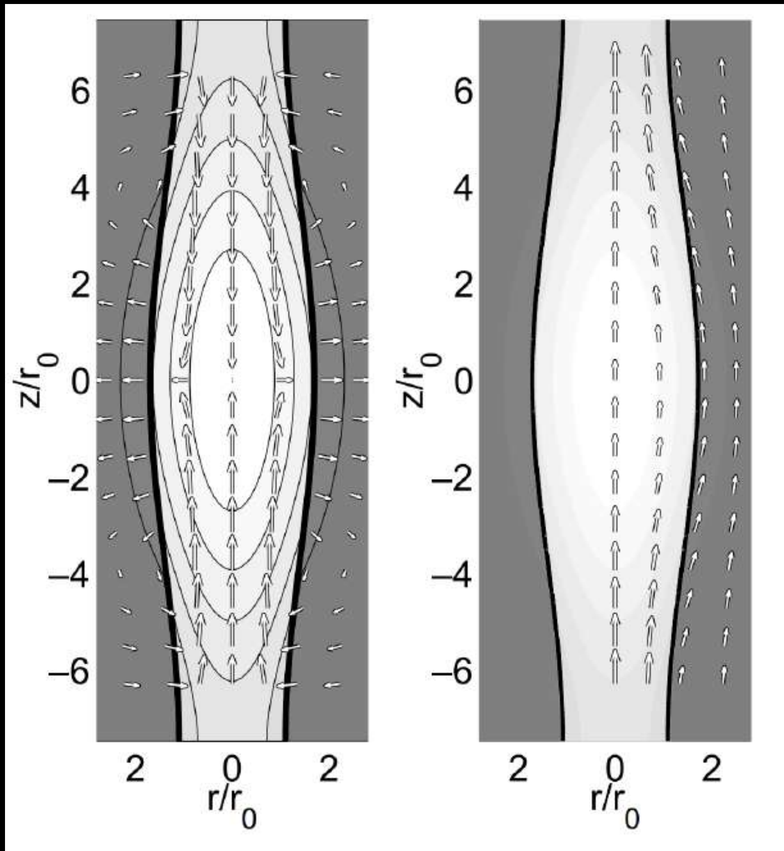

Fiege & Pudritz (2000b)

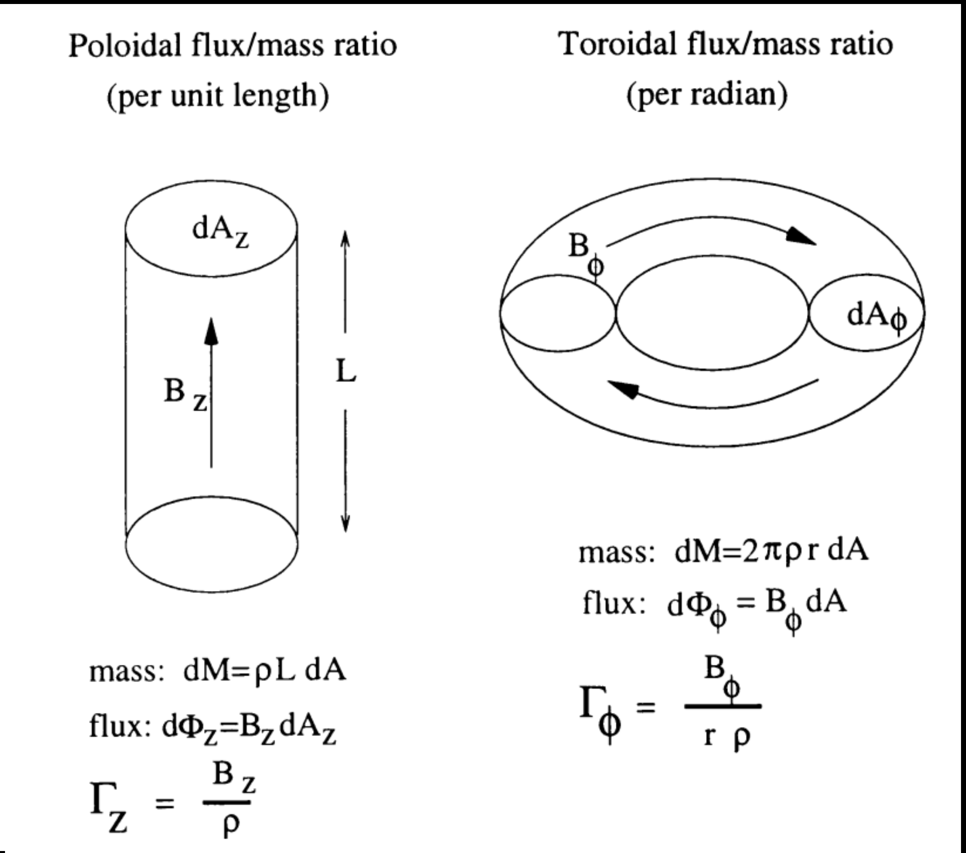

Fiege & Pudritz (2000a)

Magnetic Field Structures in Filamentary Clouds

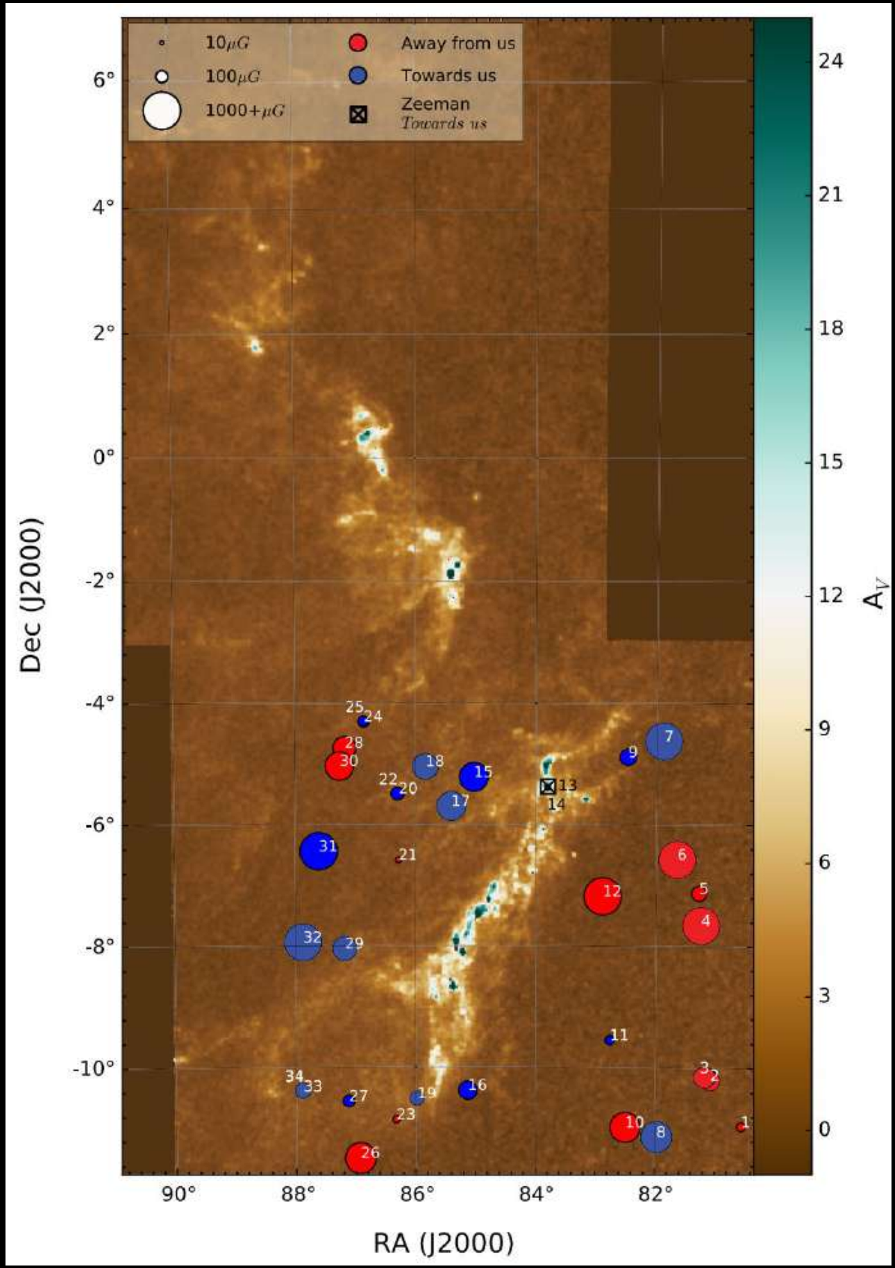

B_{LOS} around ORION A
(Tahani et al. 2018)

Helical field around
filamentary clouds?

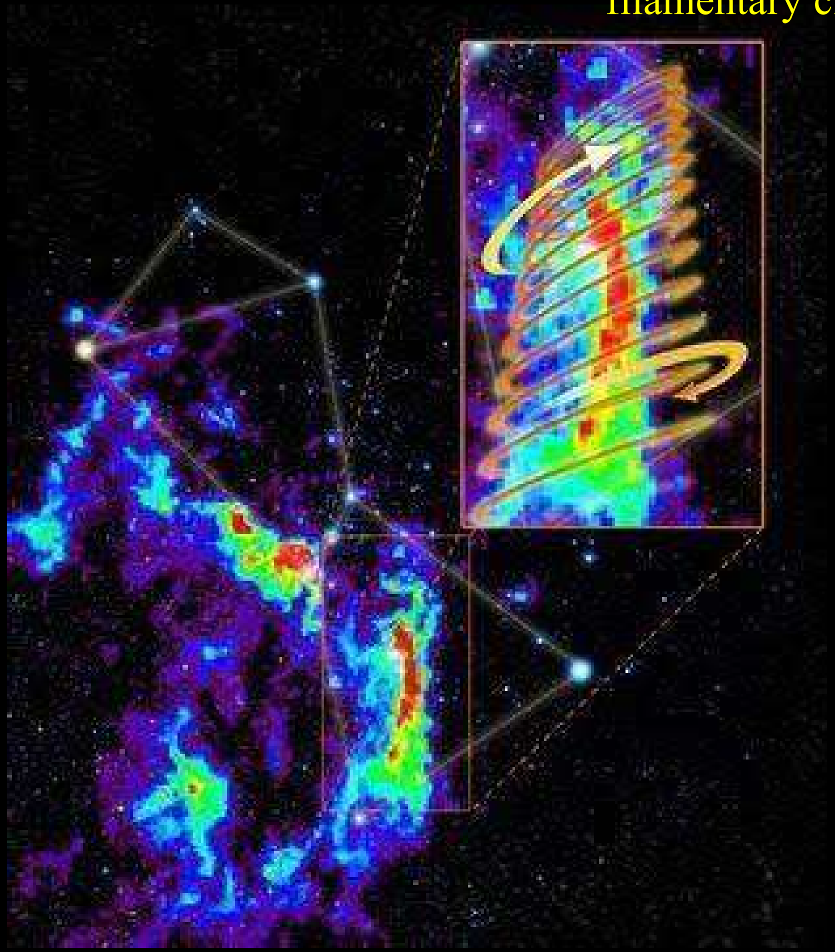

Magnetic Field Structures in Filamentary Clouds

^{13}CO emission image of Taurus cloud complex

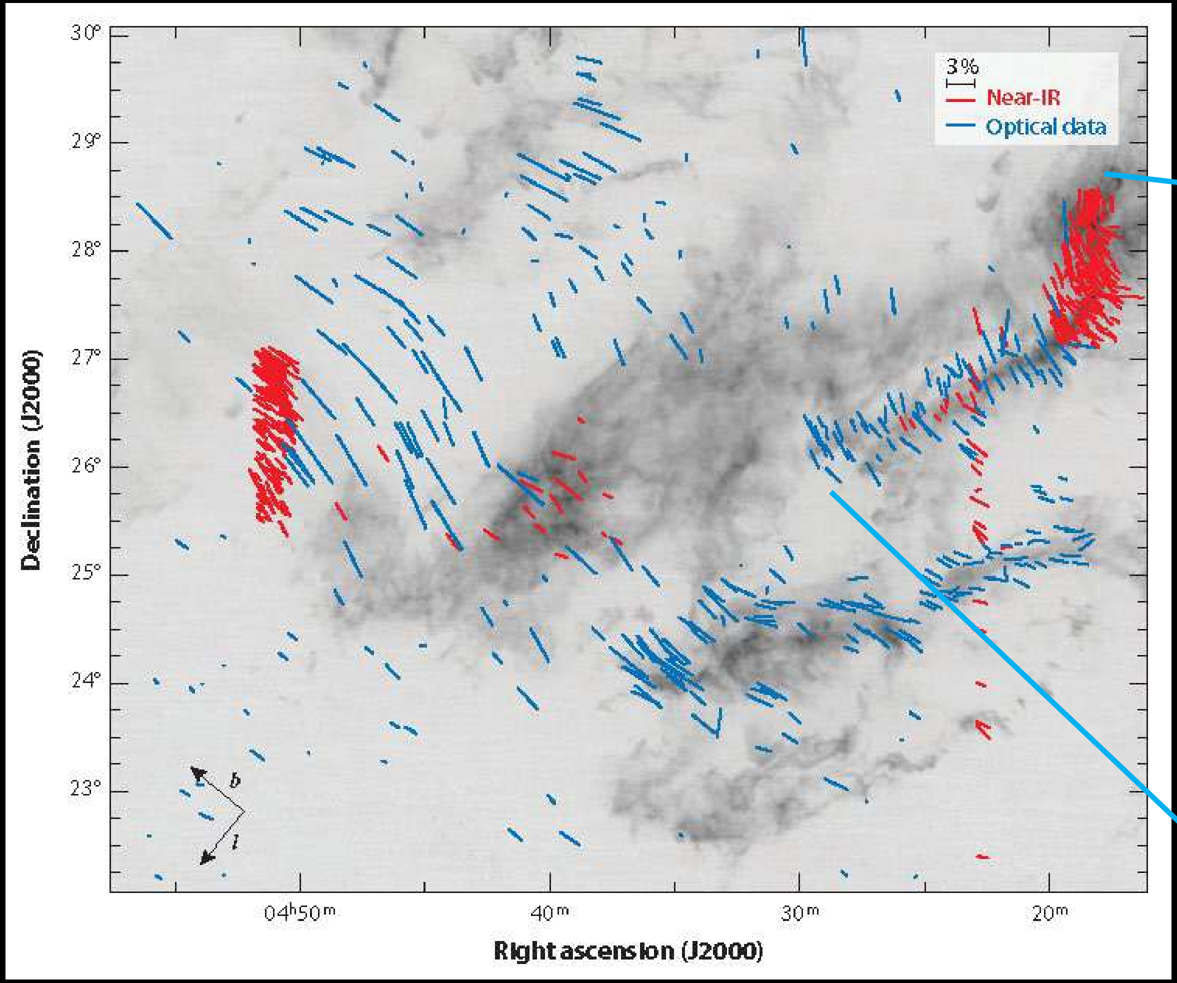

filamentary cloud L1495/B7-218

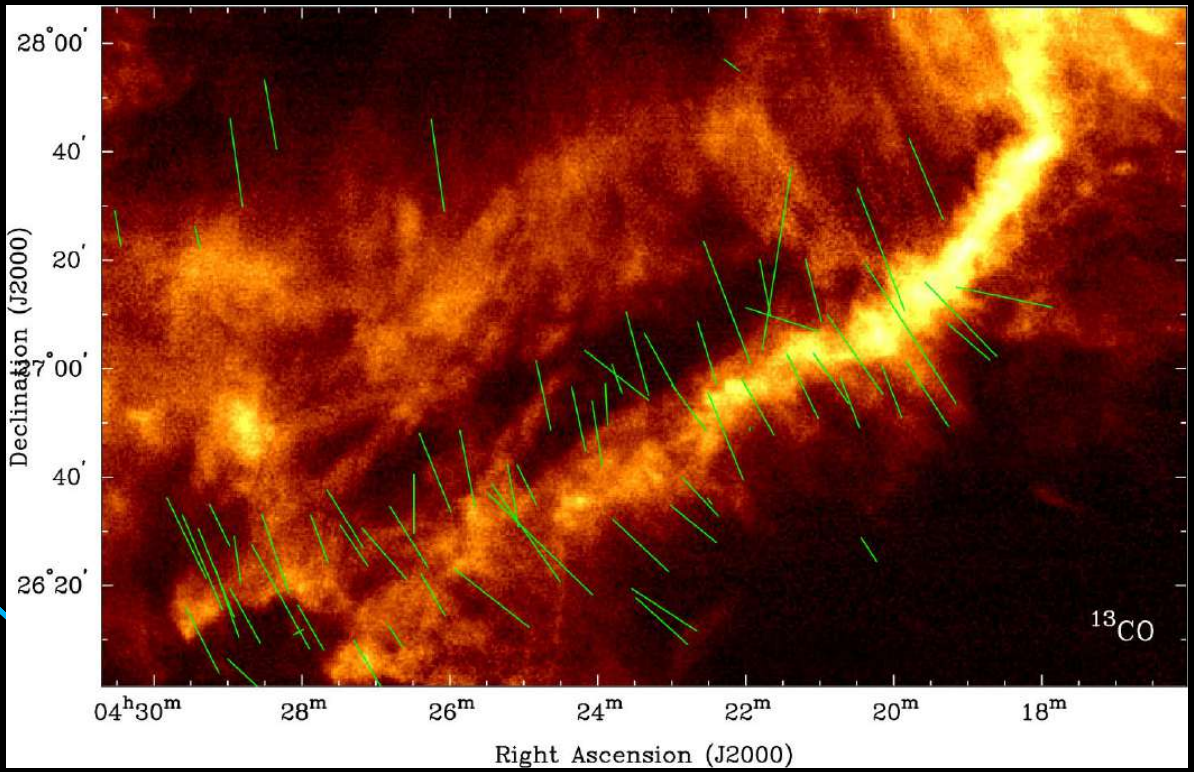

Chapman et al. (2011)

Magnetic Field Structures in Filamentary Clouds

OMC-1 in Orion A (Pattle et al. 2017)

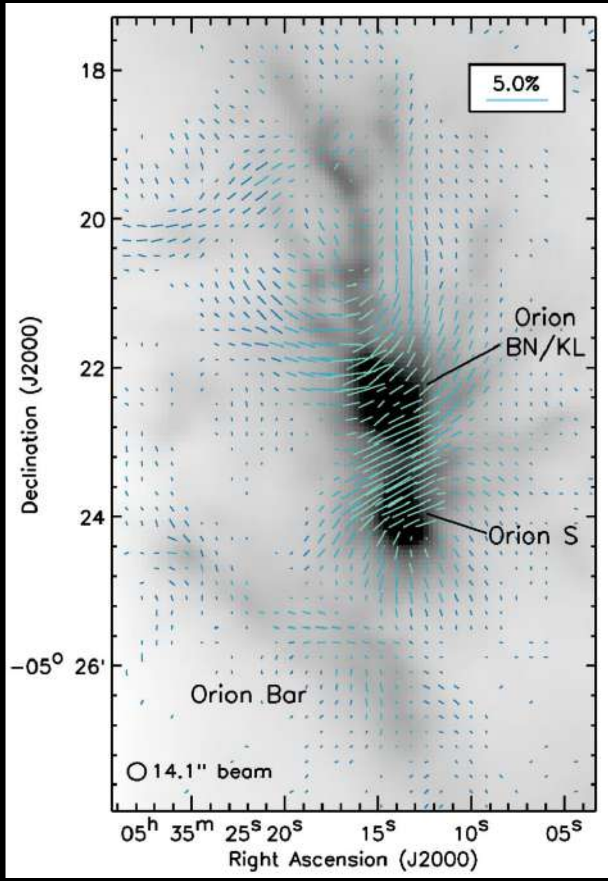

$B_{POS} \sim 6.6$ mG

G34.43+0.24 (Soam et al. 2019)

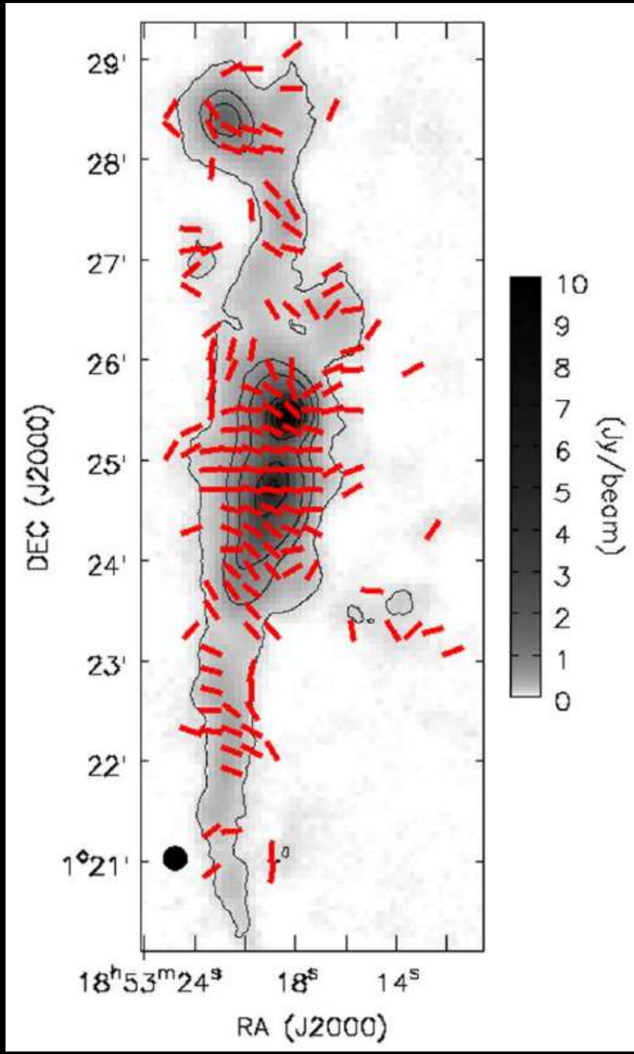

$B_{POS} = 60 \sim 470$ μG

G47.06+0.26 (Stephen et al. 2022)

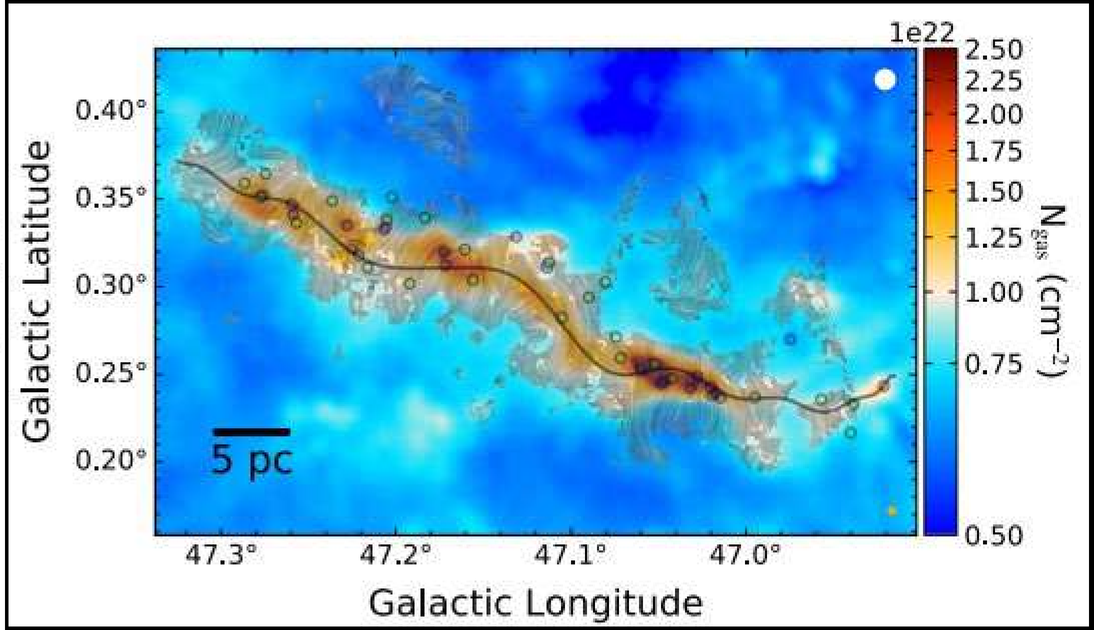

$B_{POS} = 20 \sim 160$ μG

Simulation of the Formation of IRDCs

Model parameters:

- Thermal Mach number $M_s = 10$
- Alfven Mach number $M_A = 1$
- Virial parameter $\alpha_{vir} = 1$

- Size L = 4.55 pc
- Total mass $M = 3110\ M_\odot$
- $n(H) = 960\ cm^{-3}$
- $t_{ff} = 0.59\ t_f = 1.4\times10^6$ yrs
- Isothermal, T = 10K
- Plasma $\beta = 0.02$
- Mass-to-flux ratio $\mu_\Phi = 1.62$
- B field strength = 31.6 μG

- 512^3 base grid
- 2 levels refinement (~460 AU)
- Periodic boundaries
- Turbulence driving at k = 1~2 at all time
- Turn on gravity after 2 crossing time t_f

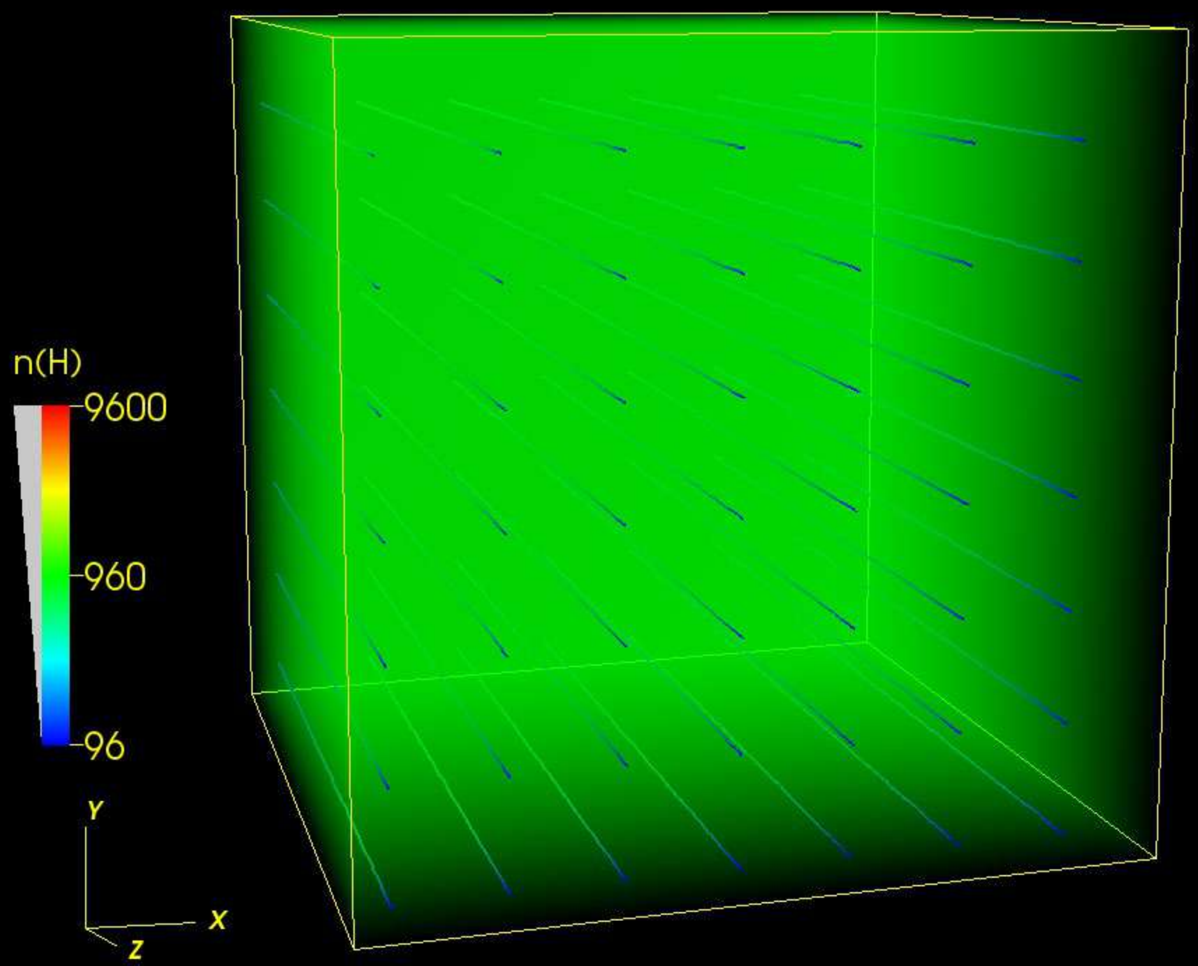

Simulation of the Formation of IRDCs

Model parameters:

- Thermal Mach number $M_s = 10$
- Alfven Mach number $M_A = 1$
- Virial parameter $\alpha_{vir} = 1$

- Size L = 4.55 pc
- Total mass $M = 3110\ M_\odot$
- $n(H) = 960\ cm^{-3}$
- $t_{ff} = 0.59\ t_f = 1.4\times10^6$ yrs
- Isothermal, T = 10K
- Plasma $\beta = 0.02$
- Mass-to-flux ratio $\mu_\Phi = 1.62$
- B field strength = 31.6 μG

- 512^3 base grid
- 2 levels refinement (~460 AU)
- Periodic boundaries
- Turbulence driving at k = 1~2 at all time
- Turn on gravity after 2 crossing time t_f

volume rendering at 0.5 t_{ff}

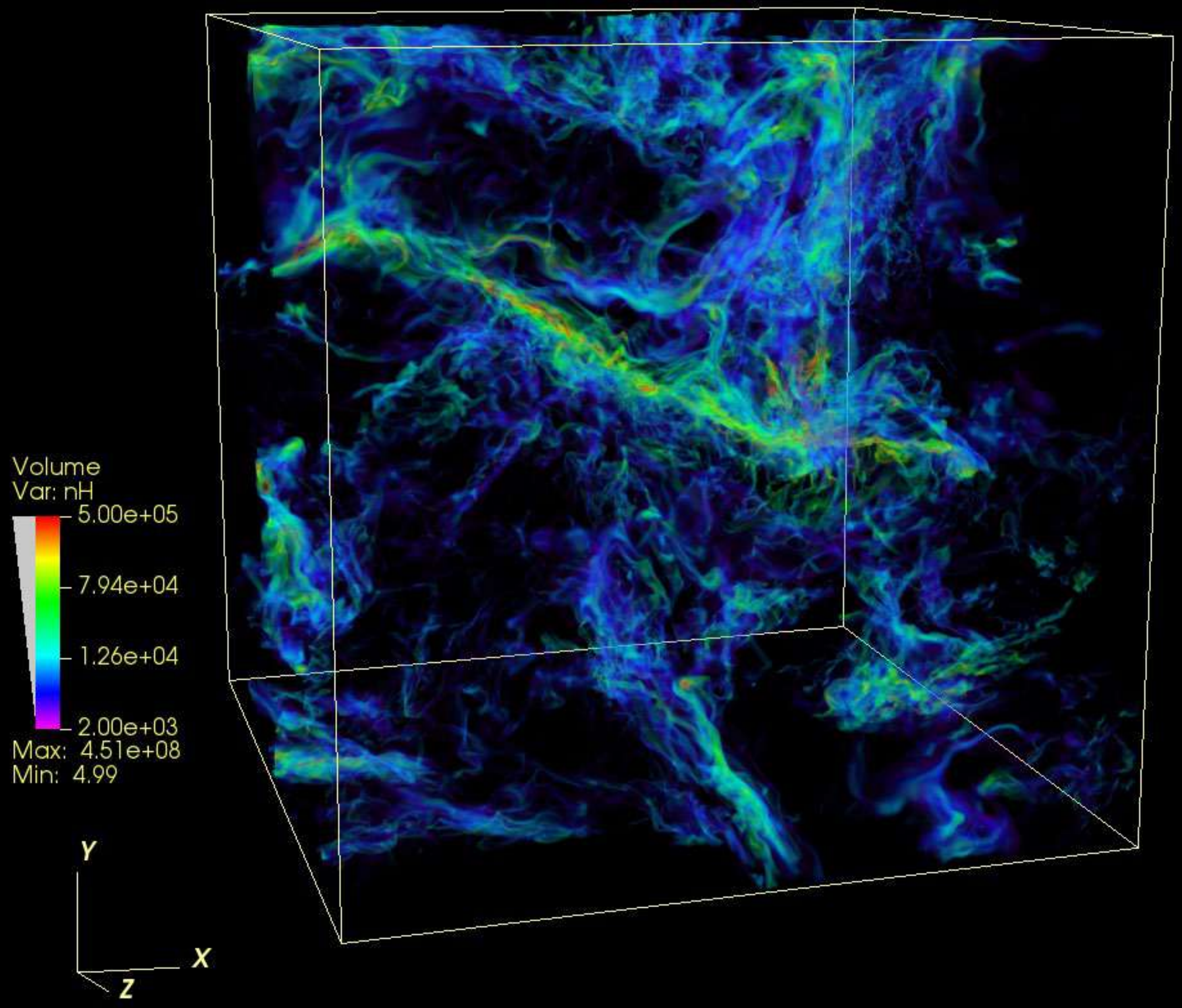

Simulation of the Formation of IRDCs

Model parameters:

- Thermal Mach number $M_s = 10$
- Alfven Mach number $M_A = 1$
- Virial parameter $\alpha_{vir} = 1$

- Size L = 4.55 pc
- Total mass $M = 3110\ M_{\odot}$
- $n(H) = 960\ cm^{-3}$
- $t_{ff} = 0.59\ t_f = 1.4\times10^6$ yrs
- Isothermal, T = 10K
- Plasma $\beta = 0.02$
- Mass-to-flux ratio $\mu_{\Phi} = 1.62$
- B field strength = 31.6 μG

- 512^3 base grid
- 2 levels refinement (~460 AU)
- Periodic boundaries
- Turbulence driving at k = 1~2 at all time
- Turn on gravity after 2 crossing time t_f

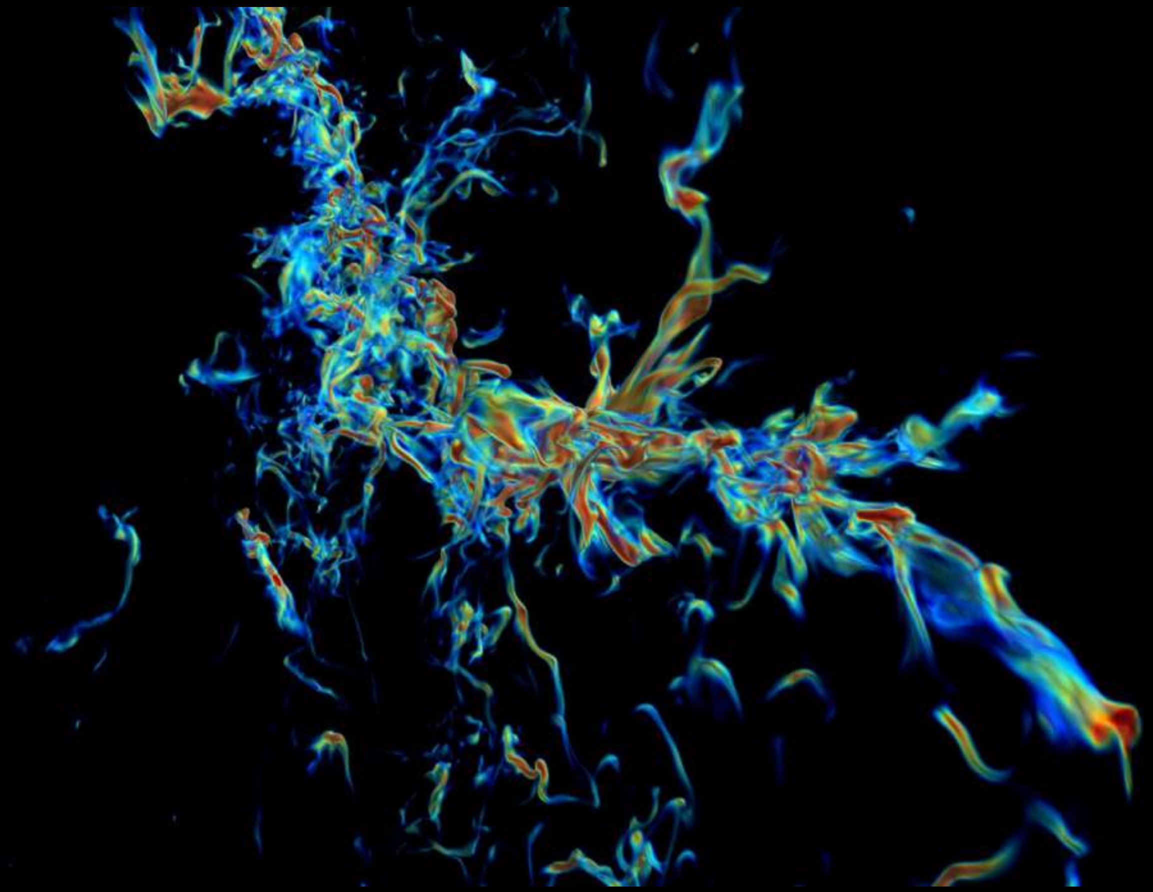

NASA Visualization Team (SC2013)

Simulation of the Formation of IRDCs

Model parameters:

- Thermal Mach number M_s = 10
- Alfven Mach number M_A = 1
- Virial parameter α_{vir} = 1

- Size L = 4.55 pc
- Total mass M = 3110 $M_\odot$
- n(H) = 960 cm^{-3}
- t_{ff} = 0.59 t_f = 1.4×10^6 yrs
- Isothermal, T = 10K
- Plasma β = 0.02
- Mass-to-flux ratio μ_Φ = 1.62
- B field strength = 31.6 μG

- 512^3 base grid
- 2 levels refinement (~460 AU)
- Periodic boundaries
- Turbulence driving at k = 1~2 at all time
- Turn on gravity after 2 crossing time t_f

getsources/getfilaments (Men'shchikov et al. 2012)

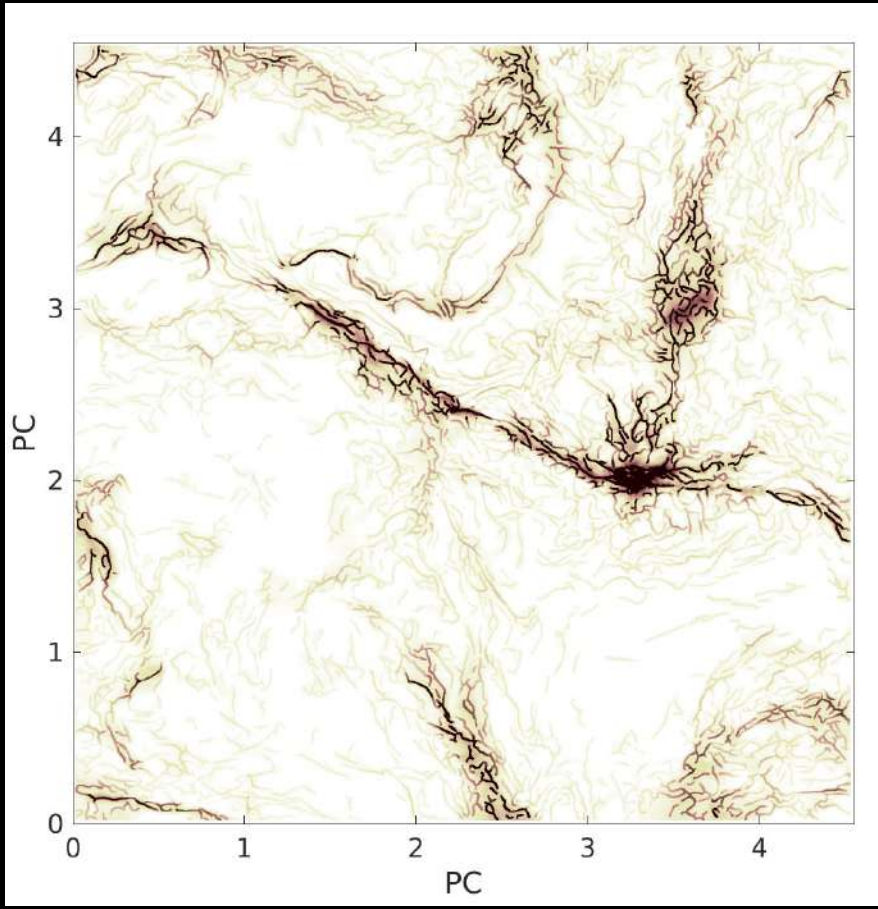

Li & Klein (2019)

Simulation of the Formation of IRDCs

Density-weighted projection of large-scale magnetic field at 0.5 t_{ff}

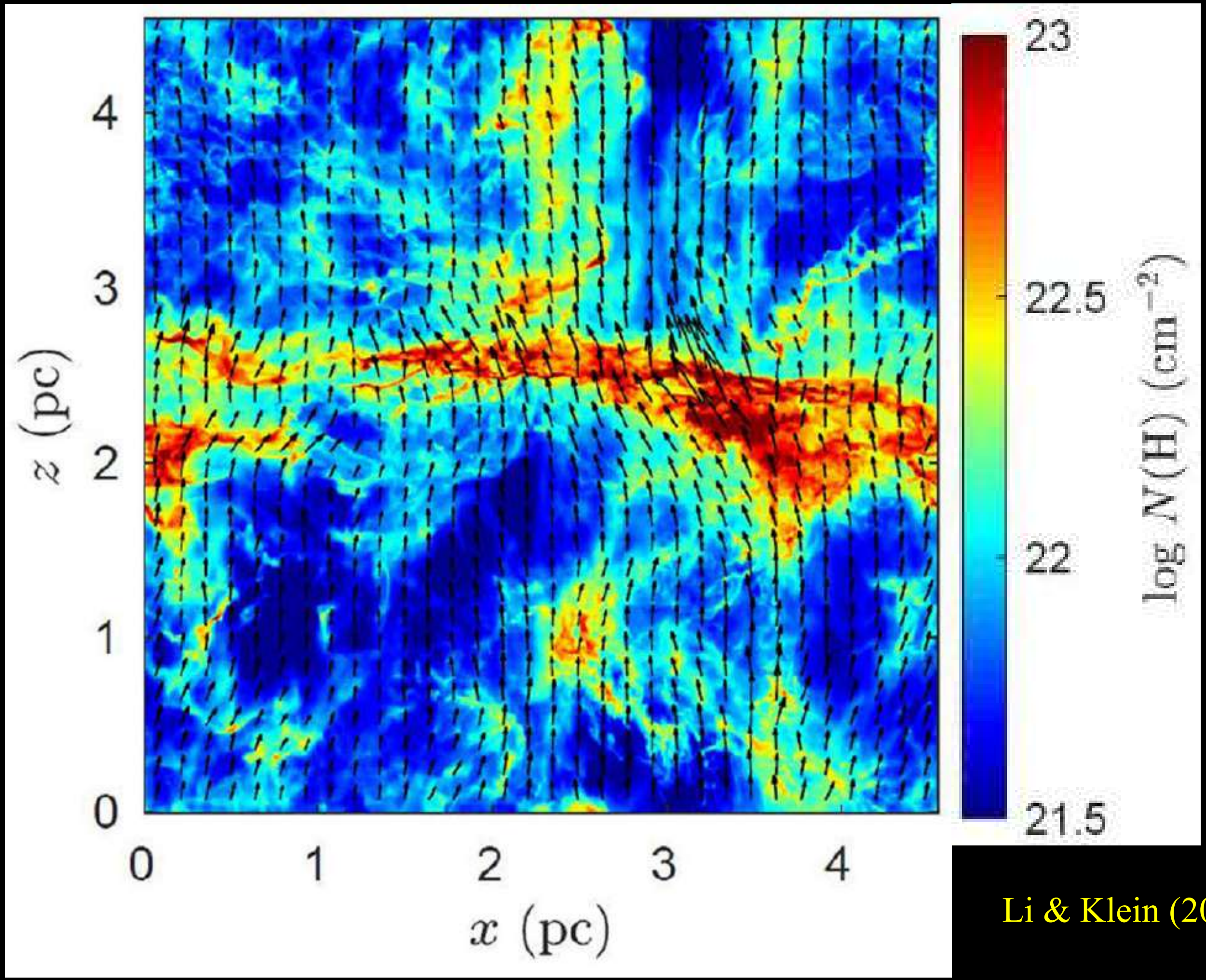

Li & Klein (2019)

Simulation of the Formation of IRDCs

3D magnetic field

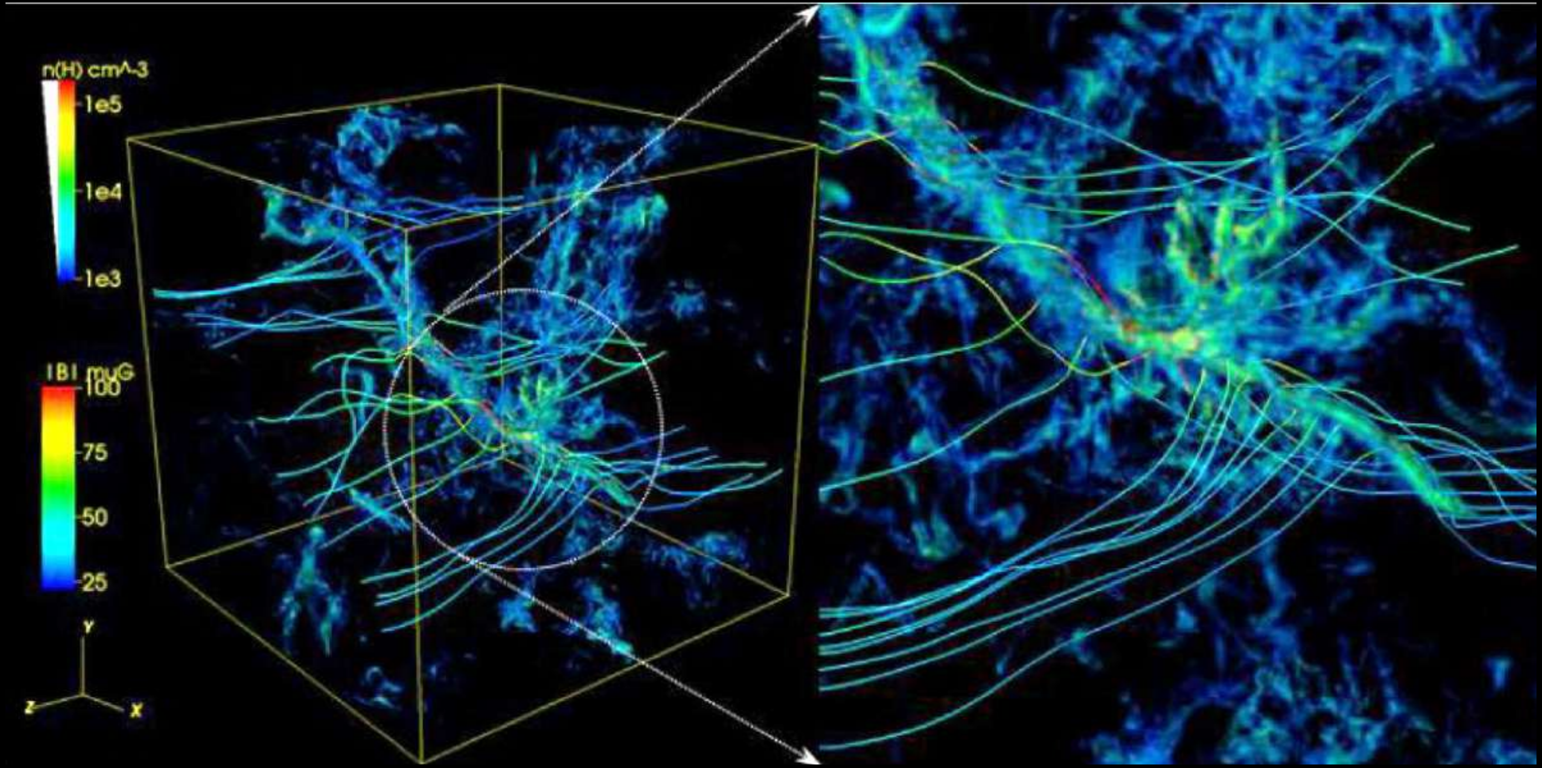

LOS magnetic field

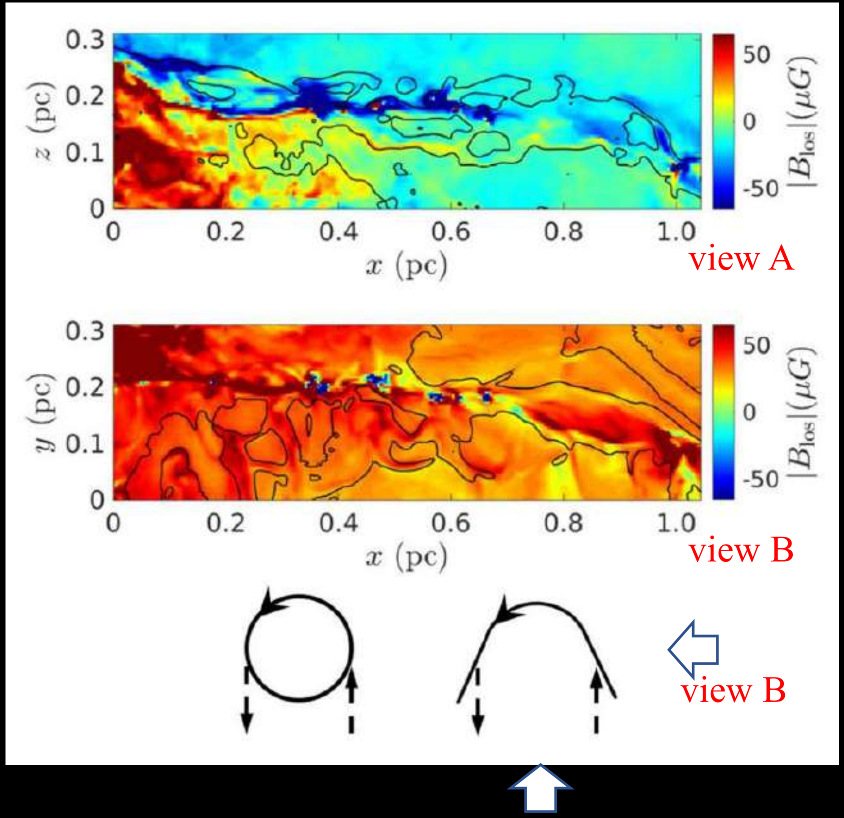

view A

Li & Klein (2019)

Simulation of the Formation of IRDCs

To form a long filamentary cloud. We need:

supersonic turbulence
+
relatively strong magnetic field
+
gravity

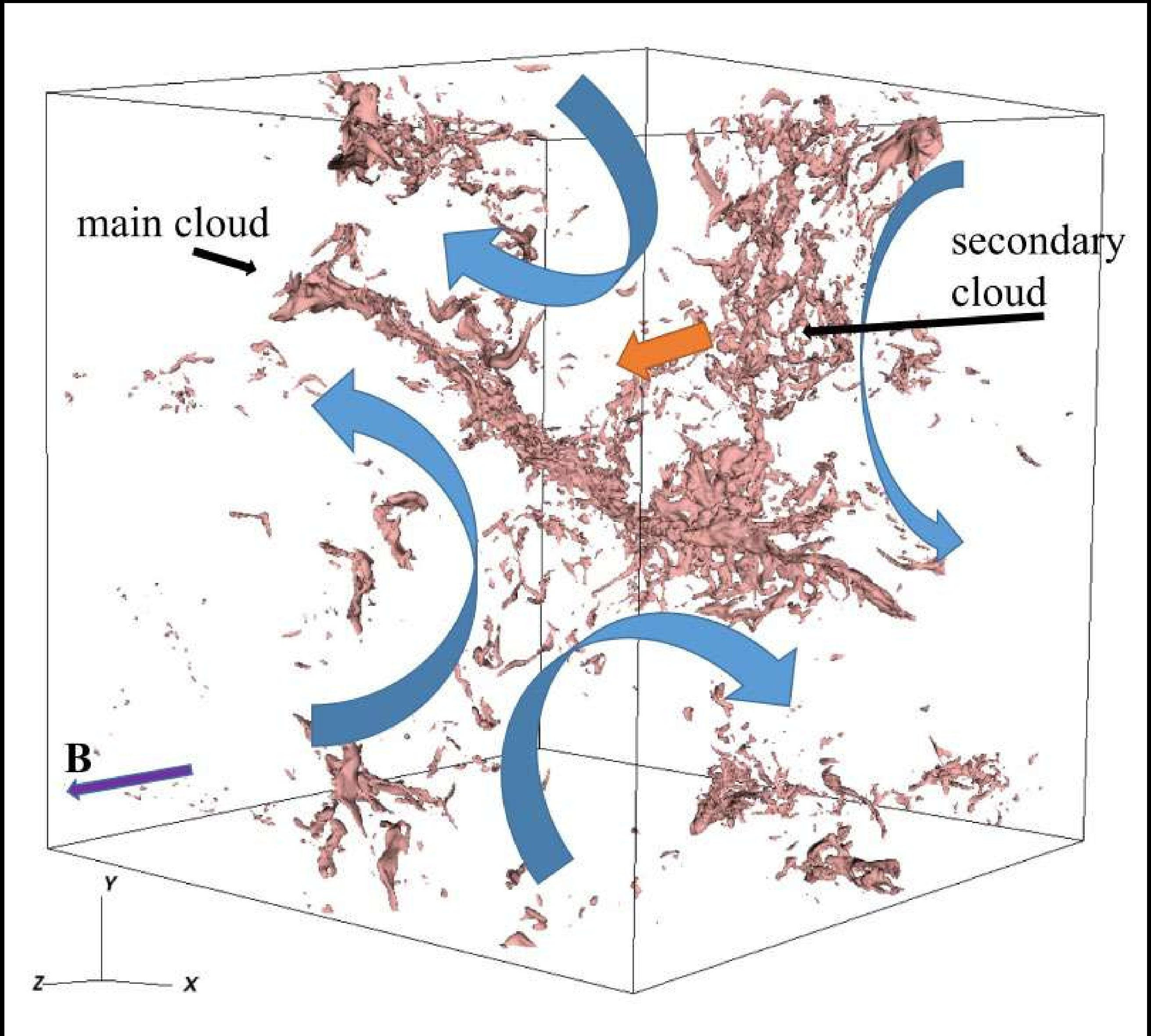

Li & Klein (2019)

Gravitational Stability of Filamentary Molecular Clouds

No magnetic field: Fiege & Pudritz (2000a)

Max mass per unit length: $M_{vir,l} = \dfrac{2\sigma_v^2}{G} \sim 16.4\ \mathrm{M_\odot\ pc^{-1}}$ if $\sigma_v = c_s$ at 10K

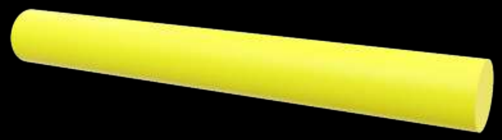

Virial parameter: $\alpha_{vir,f} = \dfrac{M_{vir,l}}{M_l} = \dfrac{2\sigma_v^2}{GM_l}$ > 1, in equilibrium

Helical magnetic field: Fiege & Pudritz (2000a)

Critical mass per unit length: $M_{\Phi,l} = \dfrac{2\sigma_v^2 + \Gamma_z^2\rho/4\pi}{G + \Gamma_\phi^2/4\pi}$

$$\Gamma_z = \frac{B_z}{\rho}, \qquad \Gamma_\phi = \frac{B_\phi}{r\rho}$$

$$\frac{M_{\Phi,l}}{M_l} > 1, \qquad \text{in equilibrium}$$

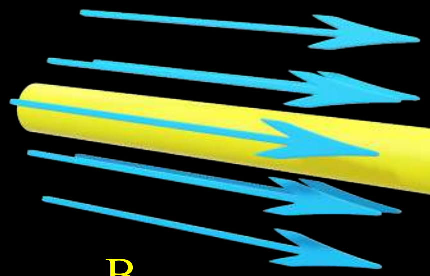

B_z

Gravitational Stability of Filamentary Molecular Clouds

Perpendicular magnetic field: Tomisaka (2014), Kasiwaki & Tomisaka (2021), Li et al. (2022a)

Critical mass per unit length: $M_{\Phi,l} = \frac{\Phi_l}{2\pi\, G^{1/2}}$

$$\mu_\Phi = \frac{M_l}{M_{\Phi,l}} = \frac{2\pi G^{1/2}\Sigma}{B_{0,3D}}$$

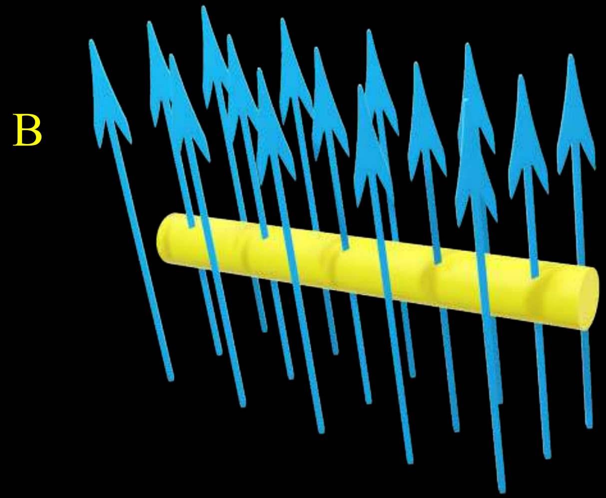

Magnetic field + thermal/turbulence motions:

$$M_{crit,l} \simeq \left(M_{\Phi,l}^2 + M_{vir,l}^2\right)^{1/2}$$

Mass per unit length in unit of critical value:

$$\frac{M_l}{M_{crit,l}} = \frac{1}{\left(\mu_\Phi^{-2} + \alpha_{vir,f}^2\right)^{1/2}}$$

< 1 for equilibrium cloud

Simulation of the Formation of IRDCs

$\frac{M_l}{M_{crit,l}} \sim 1.4,$ gravitational unstable

Li & Klein (2019)

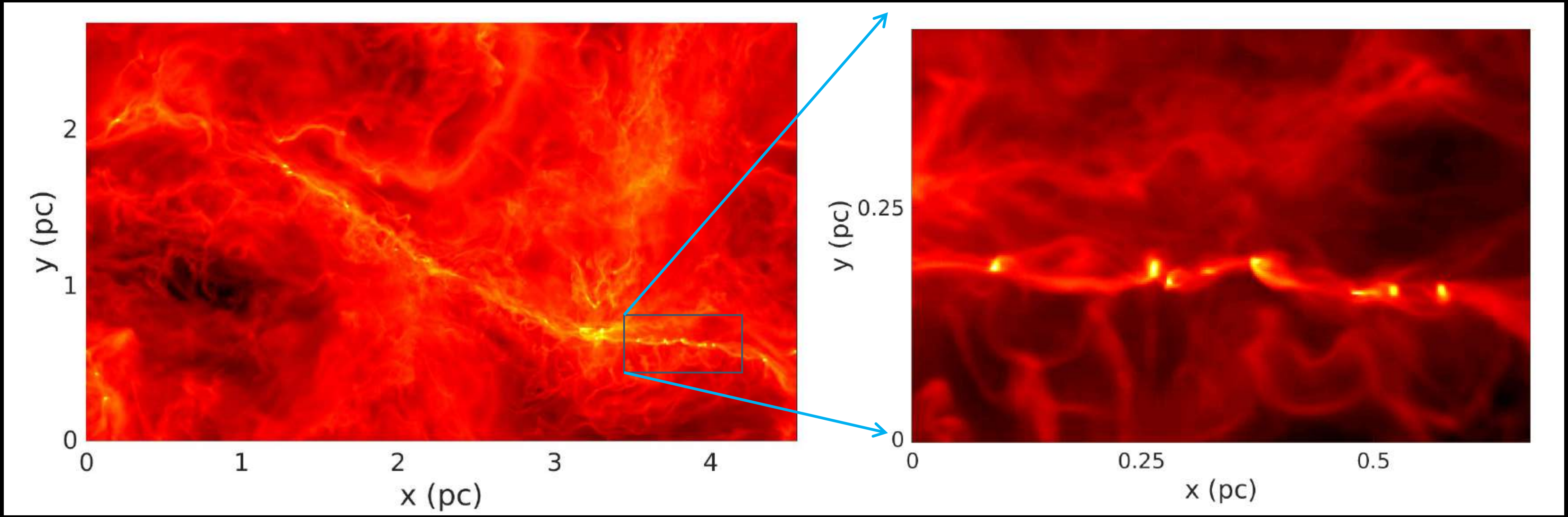

SOFIA HAWC+ (214μm) Observation of OMC-3 and OMC-4 in Orion A

C^{18}O(1-0) map of Orion A (Yun et al. 2021)

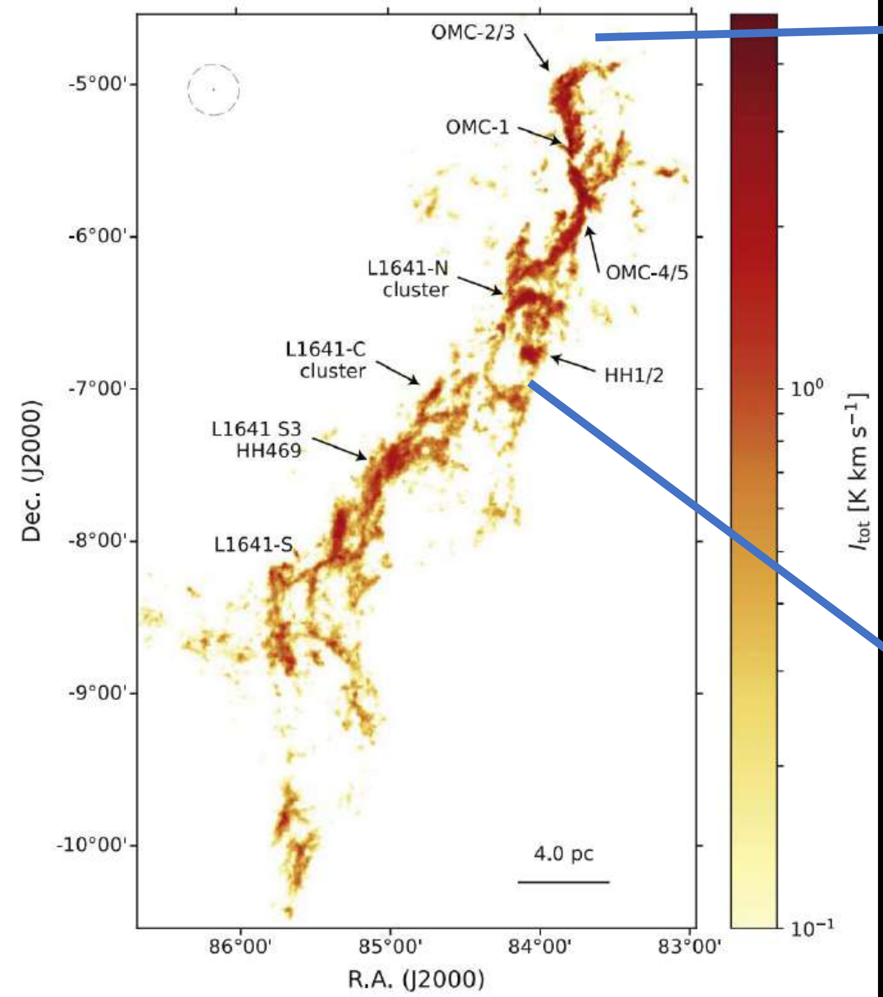

Orion integral-shaped filament C^{18}O(1-0) (Kong et al. 2018)

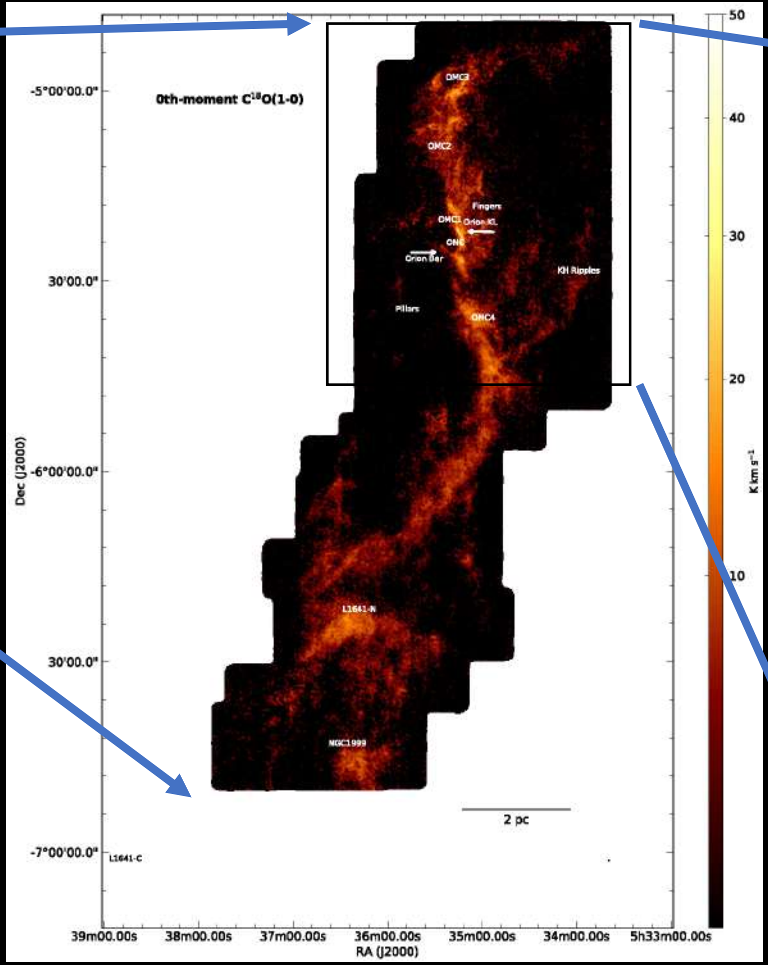

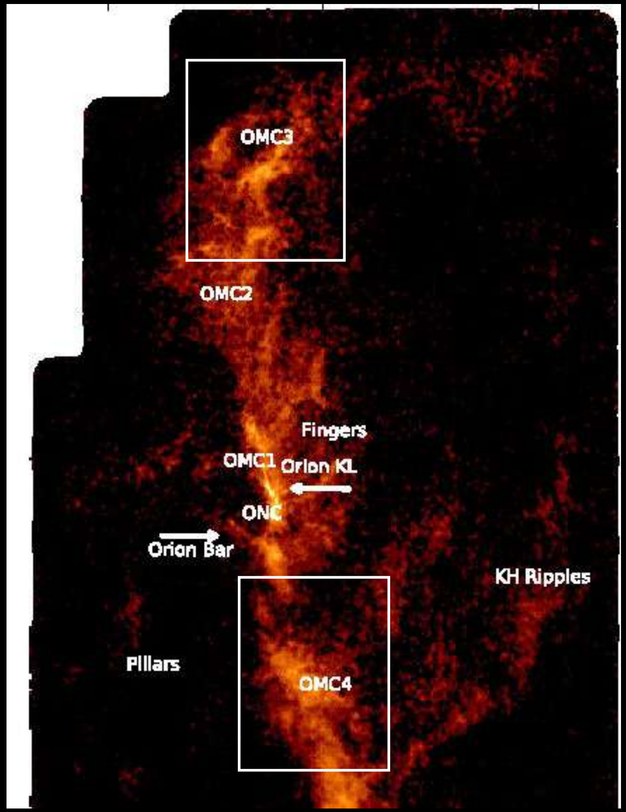

Inferred Magnetic Fields of OMC-3 and OMC-4 from SOFIA HAWC+ (Band E)

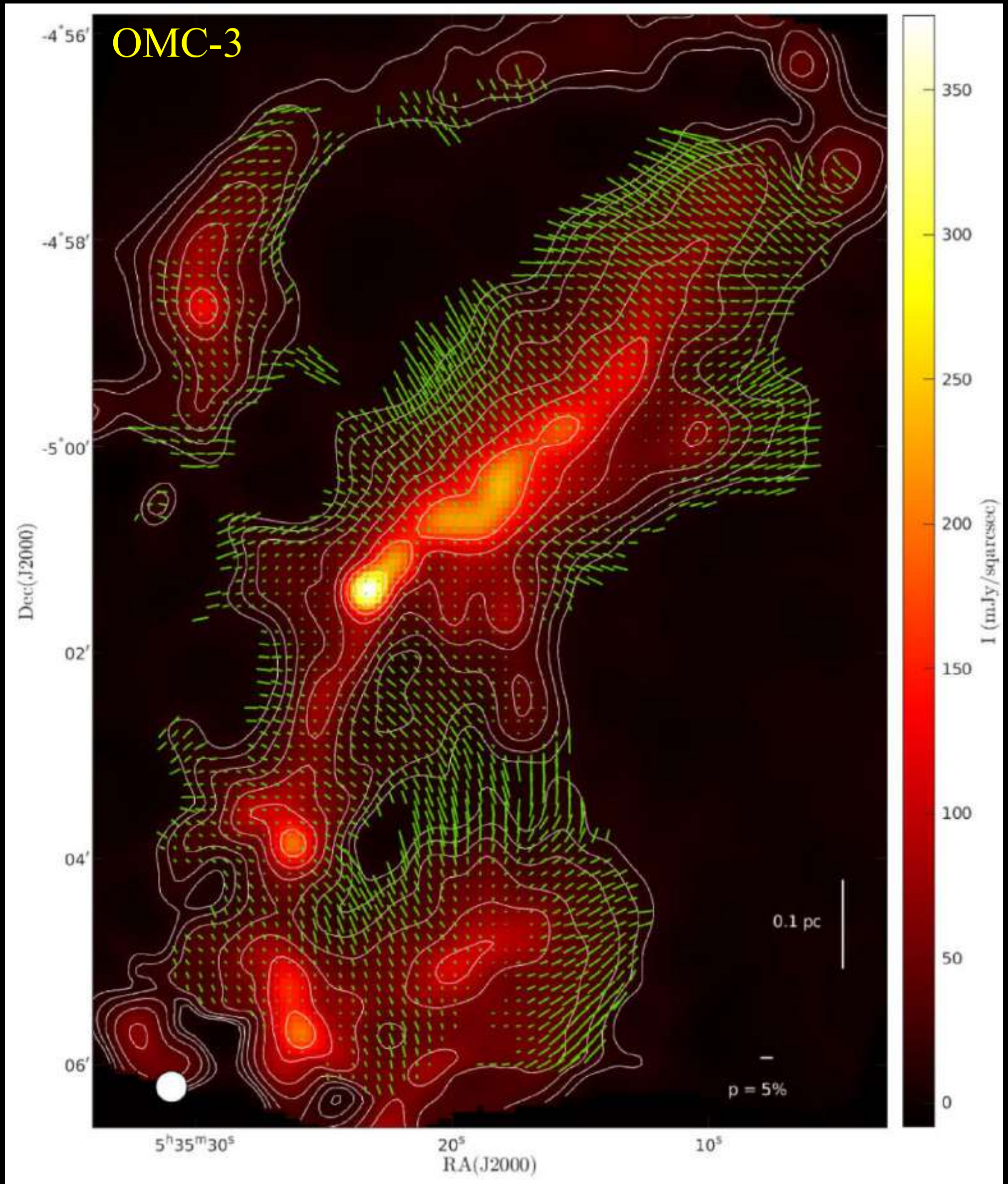

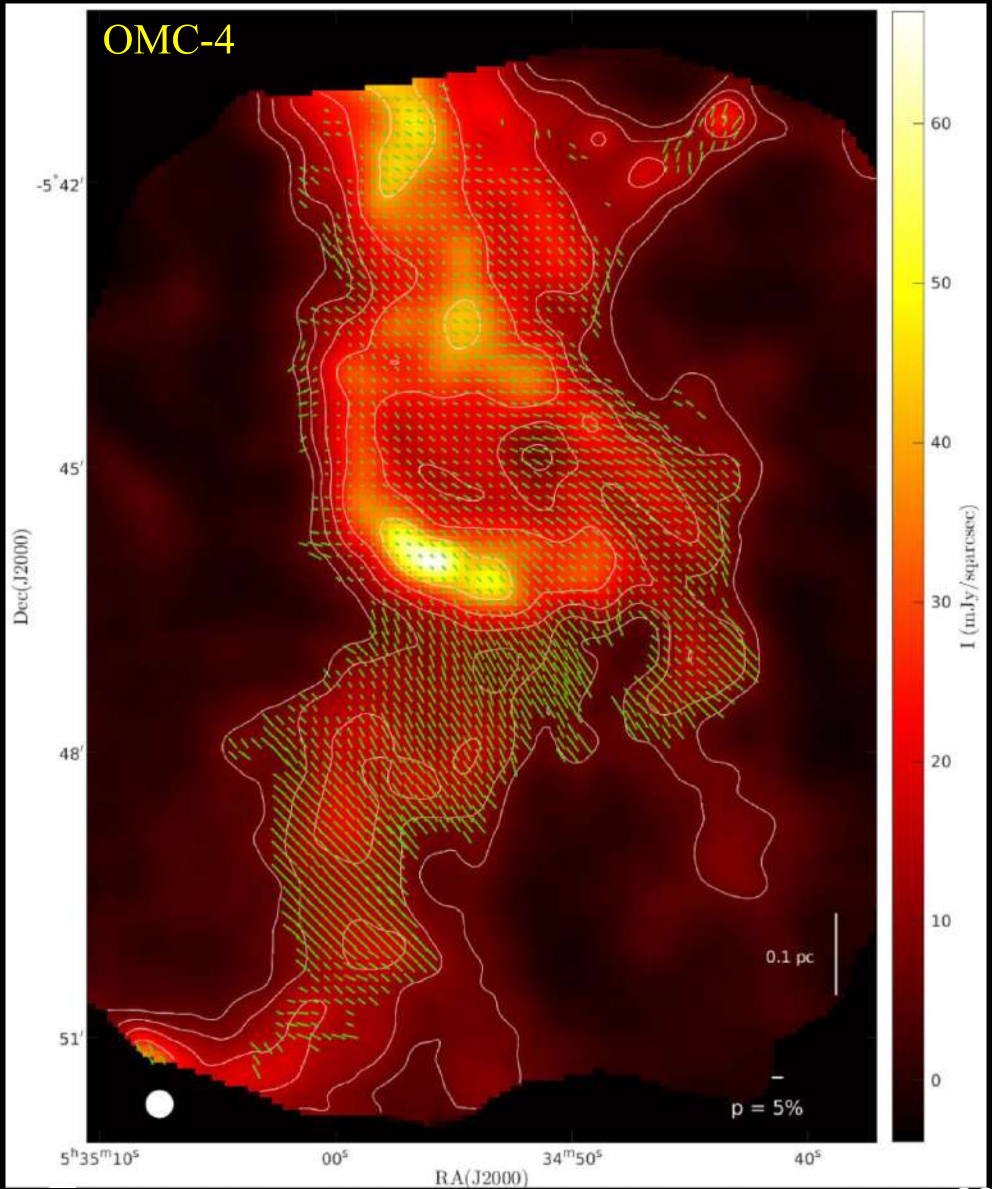

Inferred Magnetic Field Map and Physical State of **OMC-3**

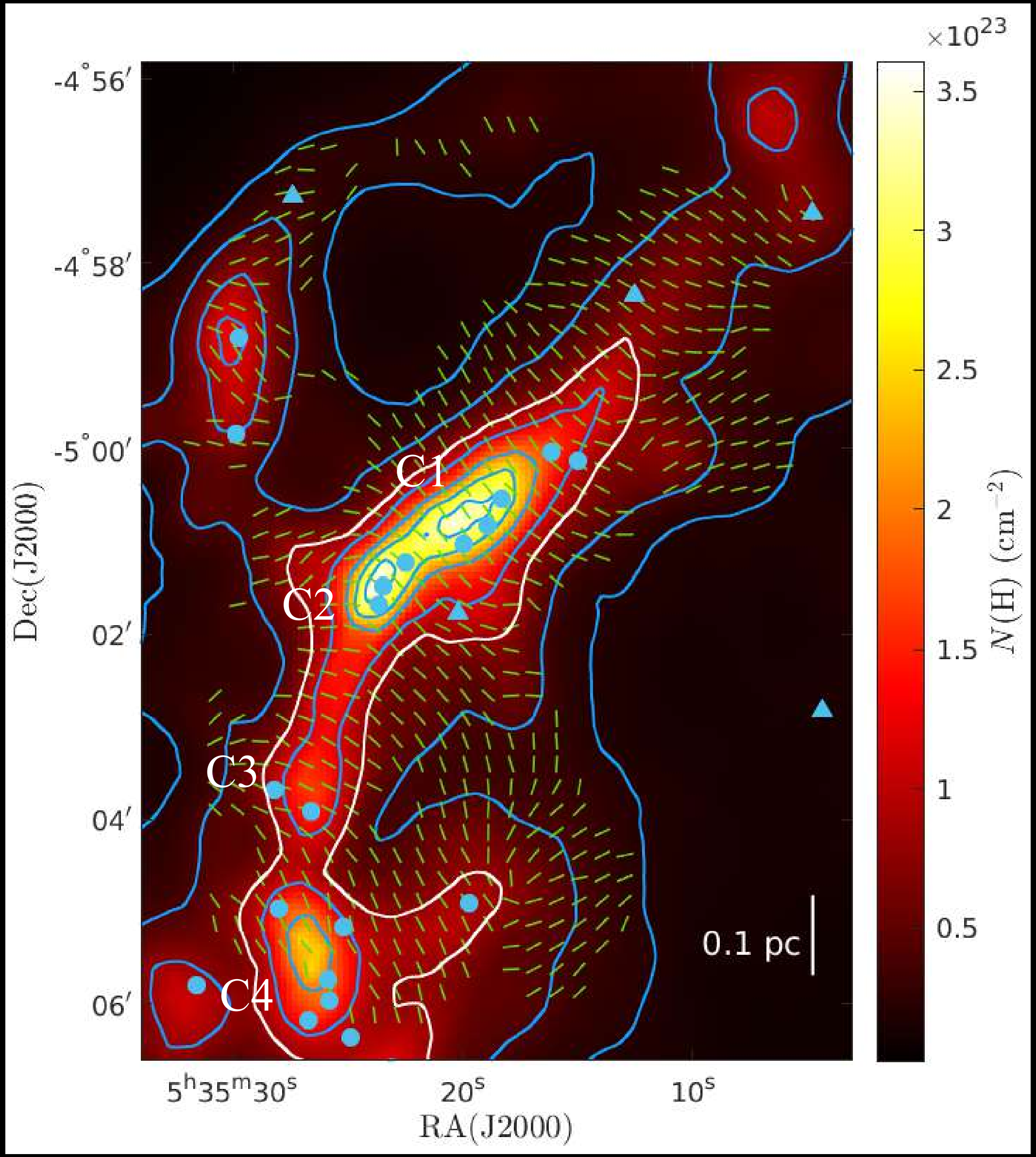

Field vector position angle distribution

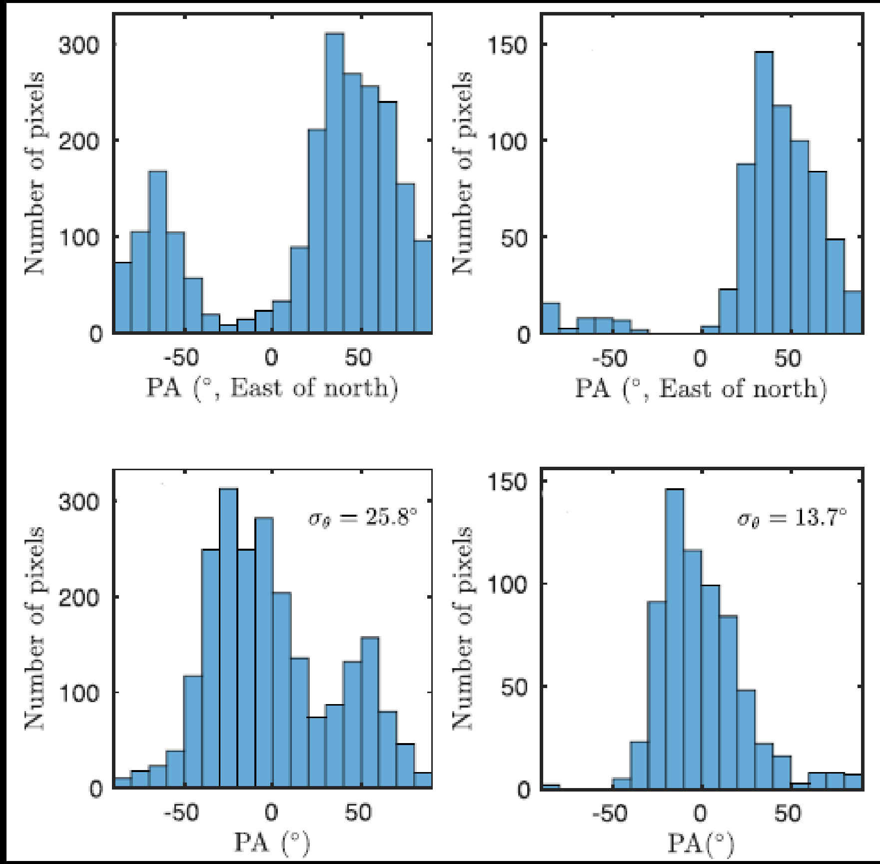

column density: Lombardi et al. (2014)

YSOs (blue circles): Furlan et al. (2016)

pre-stellar cores (blue triangles): Salji et al. (2015)

Inferred Magnetic Field Map and Physical State of **OMC-3**

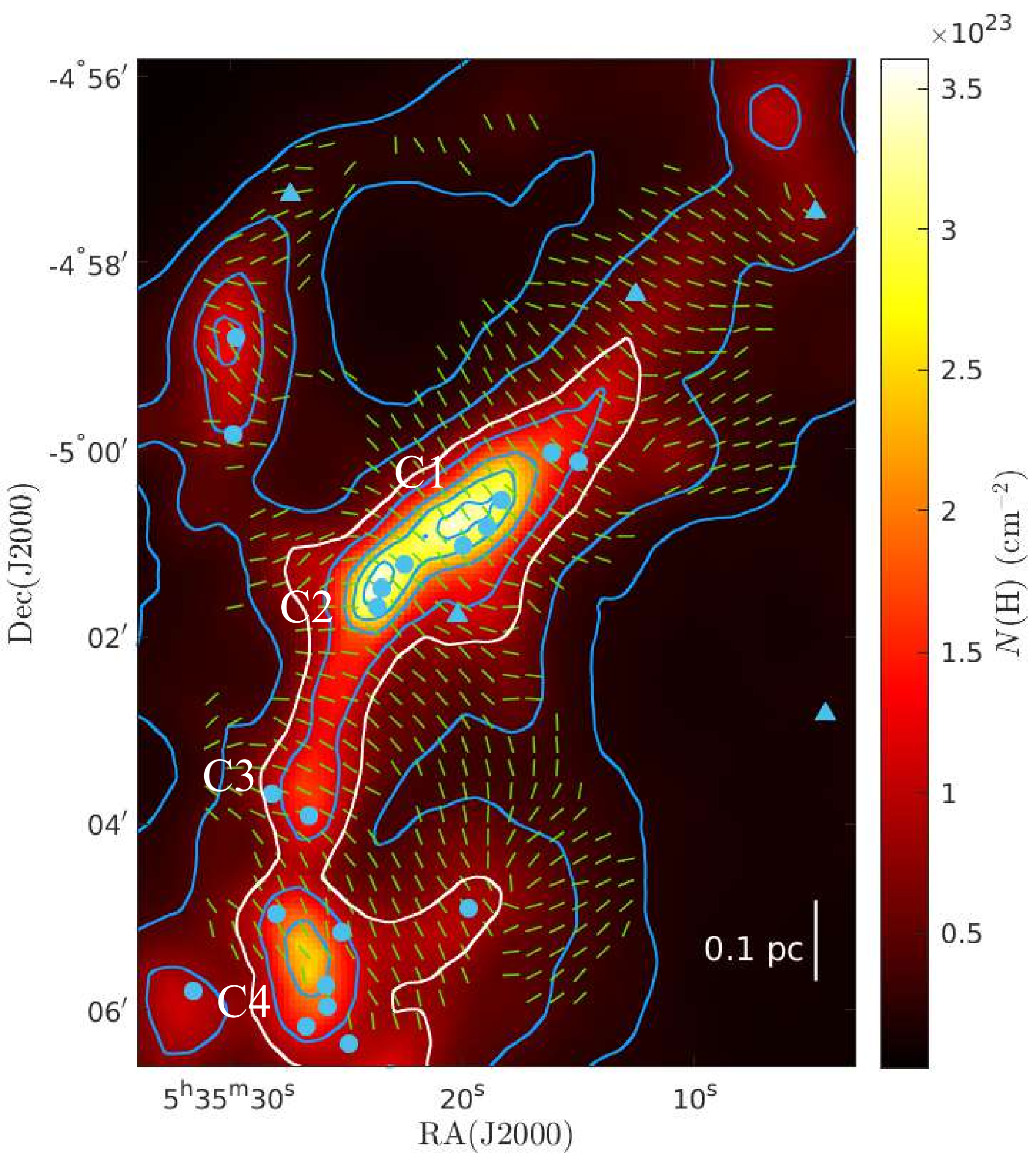

Physical state: column density: Lombardi et al. (2014)
velocity dispersion: $C^{18}O$ (1-0) Kong et al. (2018)
POS magnetic field: HAWC+ Li et al. (2022b)

Davis–Chandrasekhar–Fermi (DCF):

$$B_0 = f_{\mathrm{DCF}} \frac{(4\pi\rho)^{1/2}\sigma_v}{\tan\sigma_\theta}$$

	Entire map	Main cloud	C1	C2	C3	C4	
N(H) (10^{23} cm^{-2})	1.27	1.86	2.38	2.70	1.51	1.85	
n(H) (10^5 cm^{-3})	1.11	4.25	5.44	6.16	3.45	4.23	
σ_v(km s^{-1})	0.36	0.40	0.43	0.35	0.36	0.24	
σ_θ(deg)	25.8	13.7	6.3	13.6	2.7	20.5	
$B_{0,\mathrm{DCF}}$(μG)	67	292	775	309	1210	112	
M_A	**1.67**	**0.84**	**0.38**	**0.84**	**0.16**	**1.30**	
α_{vir}	**0.16**	**0.33**	**0.36**	**0.30**	**1.13**	**0.38**	strongly subvirial
$\mu_{\Phi,POS}$	**5.1**	**2.2**	**1.1**	**3.0**	**0.5**	**5.0**	magnetically supercritical
$M_\ell/M_{\ell,crit}$	**4.0**	**1.8**	-	-	-	-	

Inferred Magnetic Field Map and Physical State of **OMC-4**

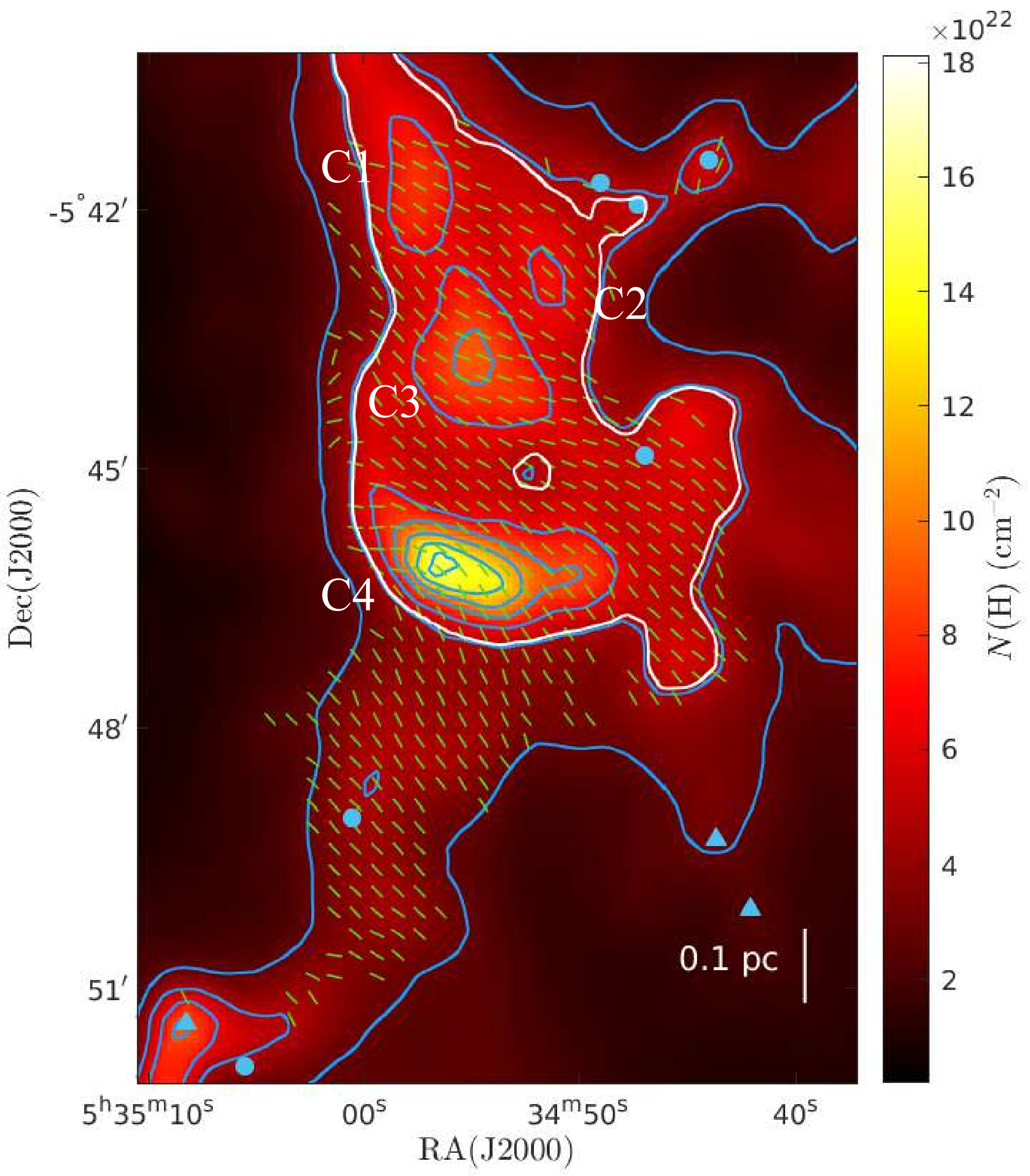

Field vector position angle distribution

entire map — main filamentary cloud

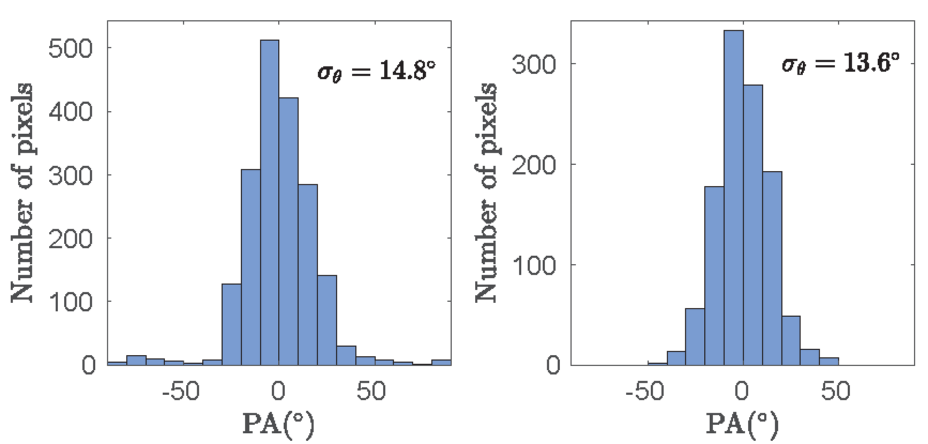

	Entire map	Main cloud	C1	C2	C3	C4
N(H) (10^{23} cm^{-2})	0.64	0.77	0.76	0.70	0.79	1.01
n(H) (10^5 cm^{-3})	0.67	0.82	0.81	0.74	0.84	1.08
σ_v(km s^{-1})	0.49	0.53	0.80	0.55	0.72	0.45
σ_θ(deg)	14.8	13.6	5.5	4.3	8.8	11.5
$B_{0,DCF}$(μG)	129	171	644	547	367	199
M_A	**0.92**	**0.84**	**0.33**	**0.26**	**0.54**	**0.71**
α_{vir}	**0.59**	**0.59**	**5.1**	**5.53**	**2.63**	**0.76**
$\mu_{\Phi,POS}$	**1.7**	**1.5**	**0.4**	**0.5**	**0.8**	**1.9**
$M_\ell/M_{\ell,crit}$	**1.2**	**1.1**	-	-	-	-

?

Histogram of Relative Orientation (HRO)

Planck collaboration XXXV (2016)

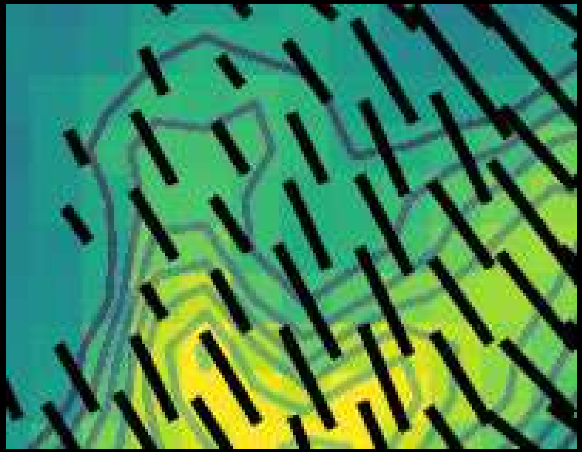

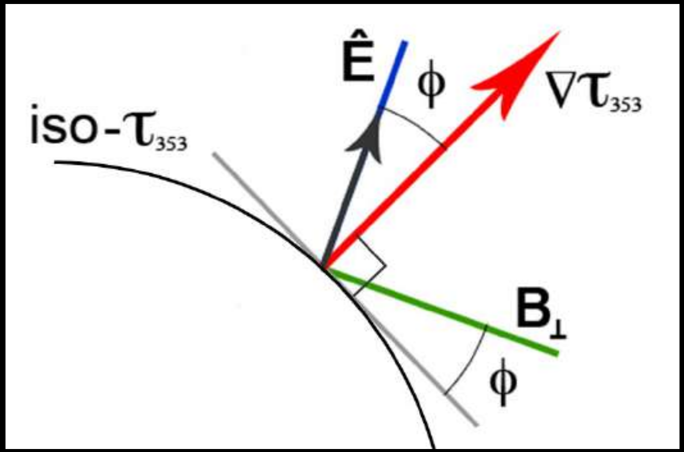

ϕ = angle between field vector and tangent of column density contour

Planck collaboration XXXV (2016)

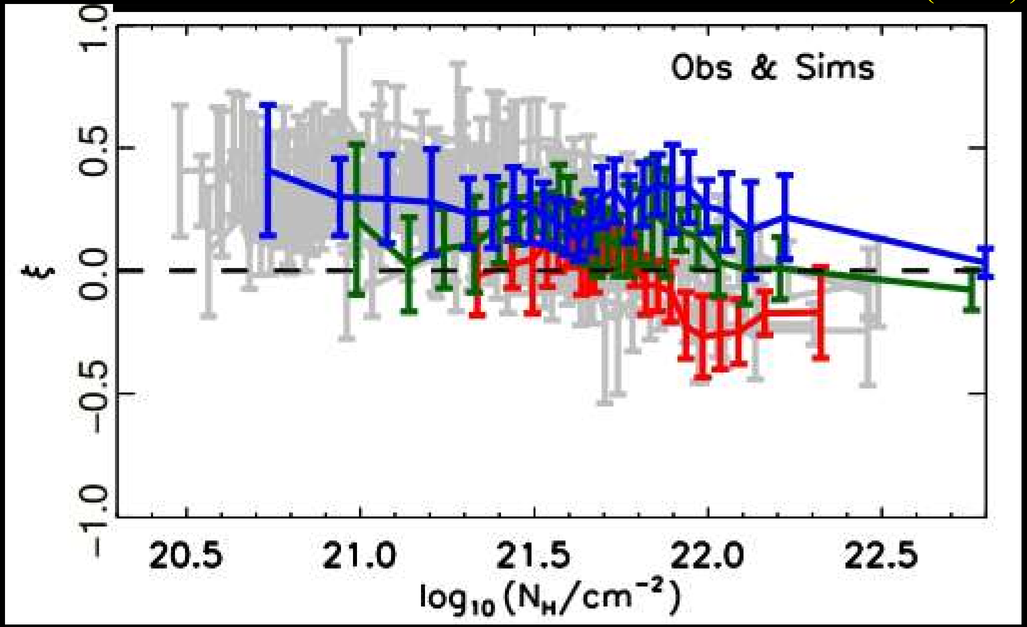

Li et al. (2022b)

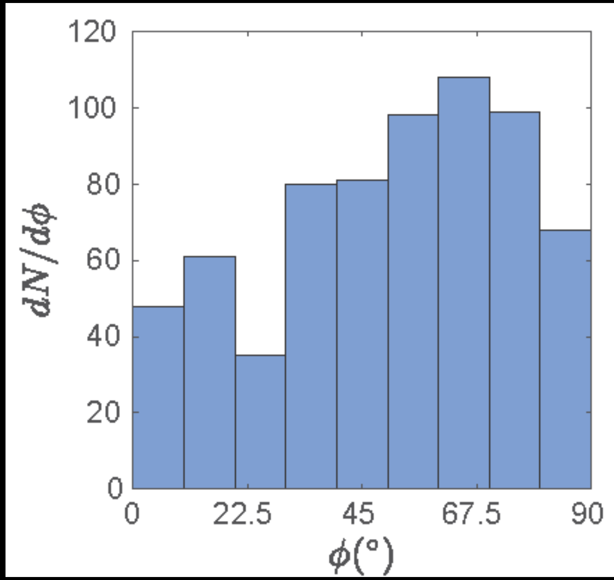

Shape Parameter:
(Soler et al. 2013, 2017)

$$\xi \equiv \frac{A_0 - A_{90}}{A_0 + A_{90}}$$

A_0 = area ($0° < \phi < 22°.5$)
A_{90} = area ($67°.5 < \phi < 90°$)

Histogram of Relative Orientation (HRO)

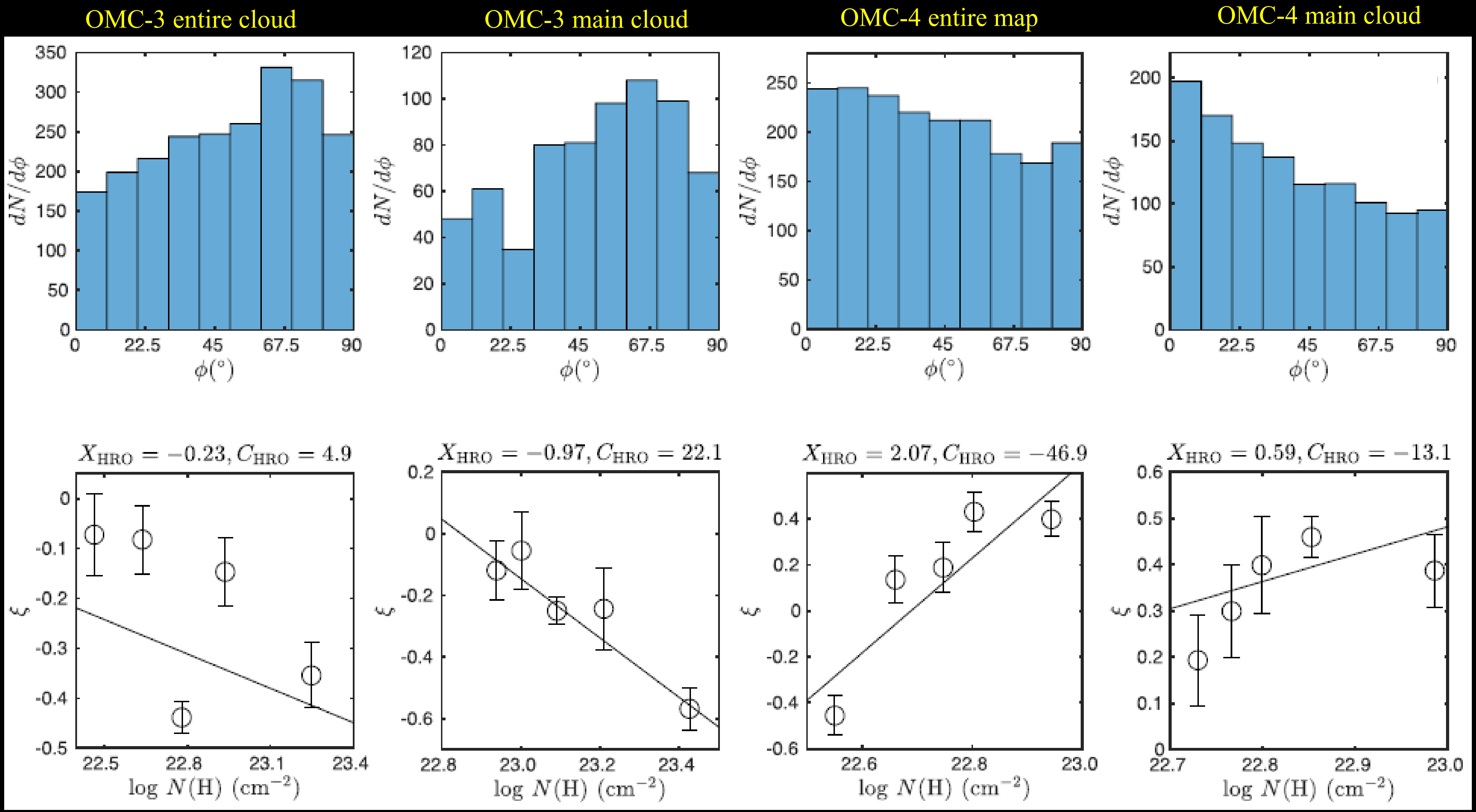

Projection Effect?

OMC-4 main cloud, ξ > 0

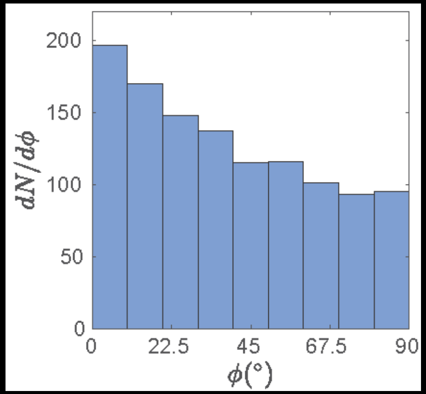

OMC-4 clump C4

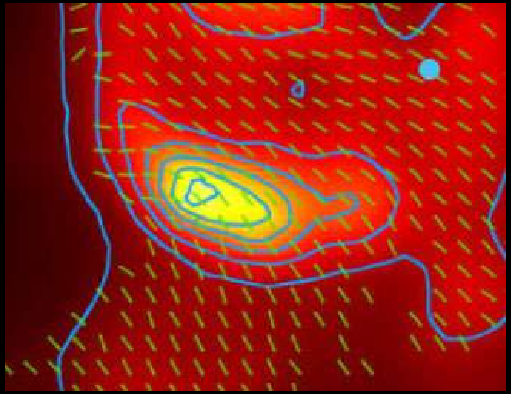

Filamentary cloud formation simulation (Li & Klein 2019, Li et al. 2022b)

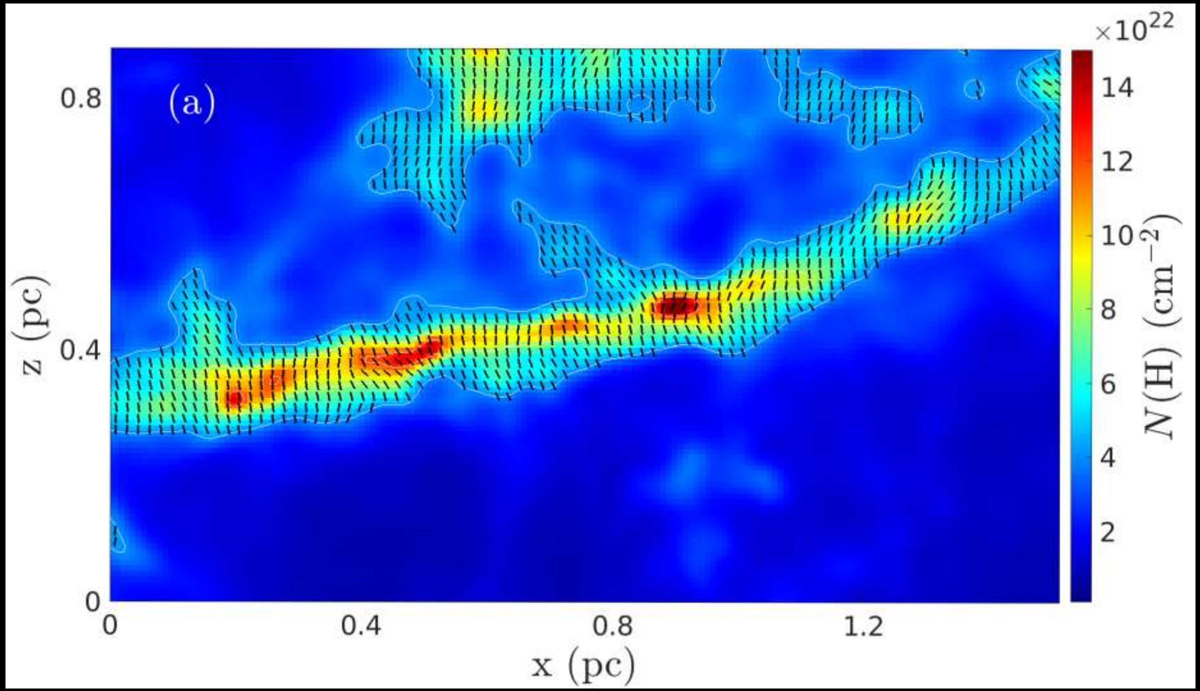

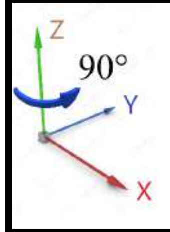

angle between filament axis and los ~ 23°

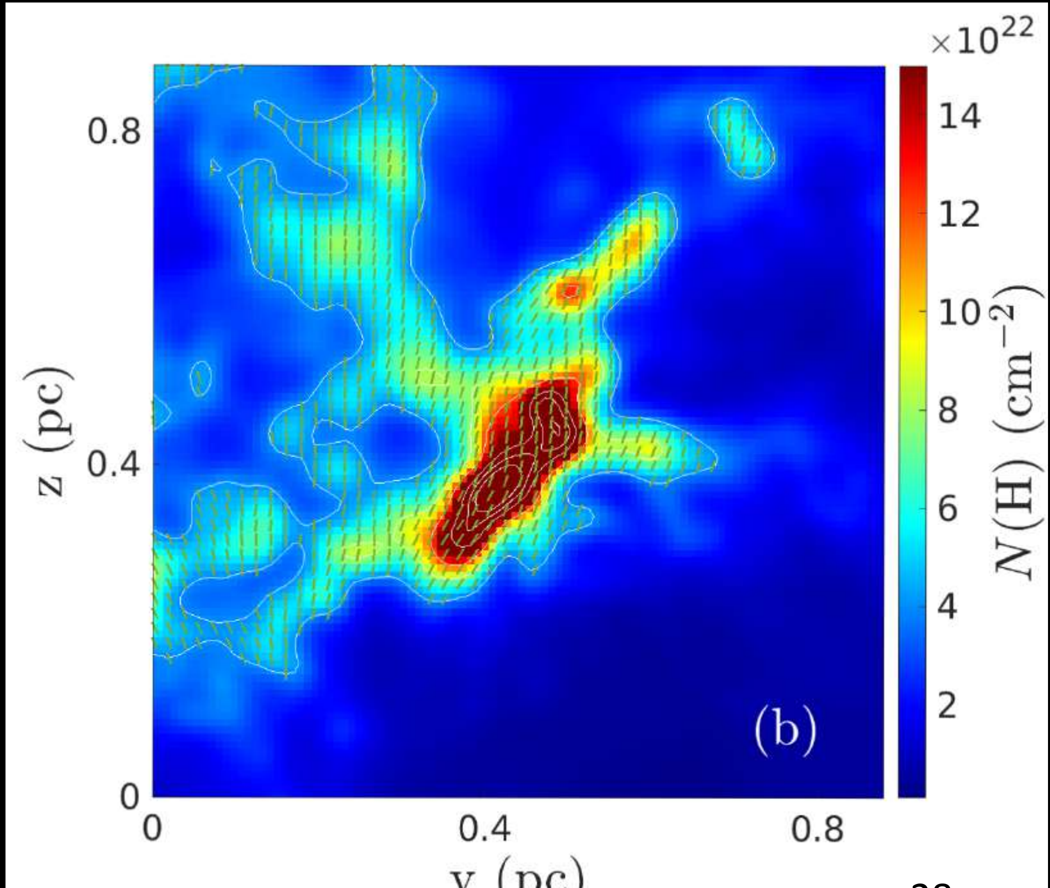

Filamentary Substructures in Orion A

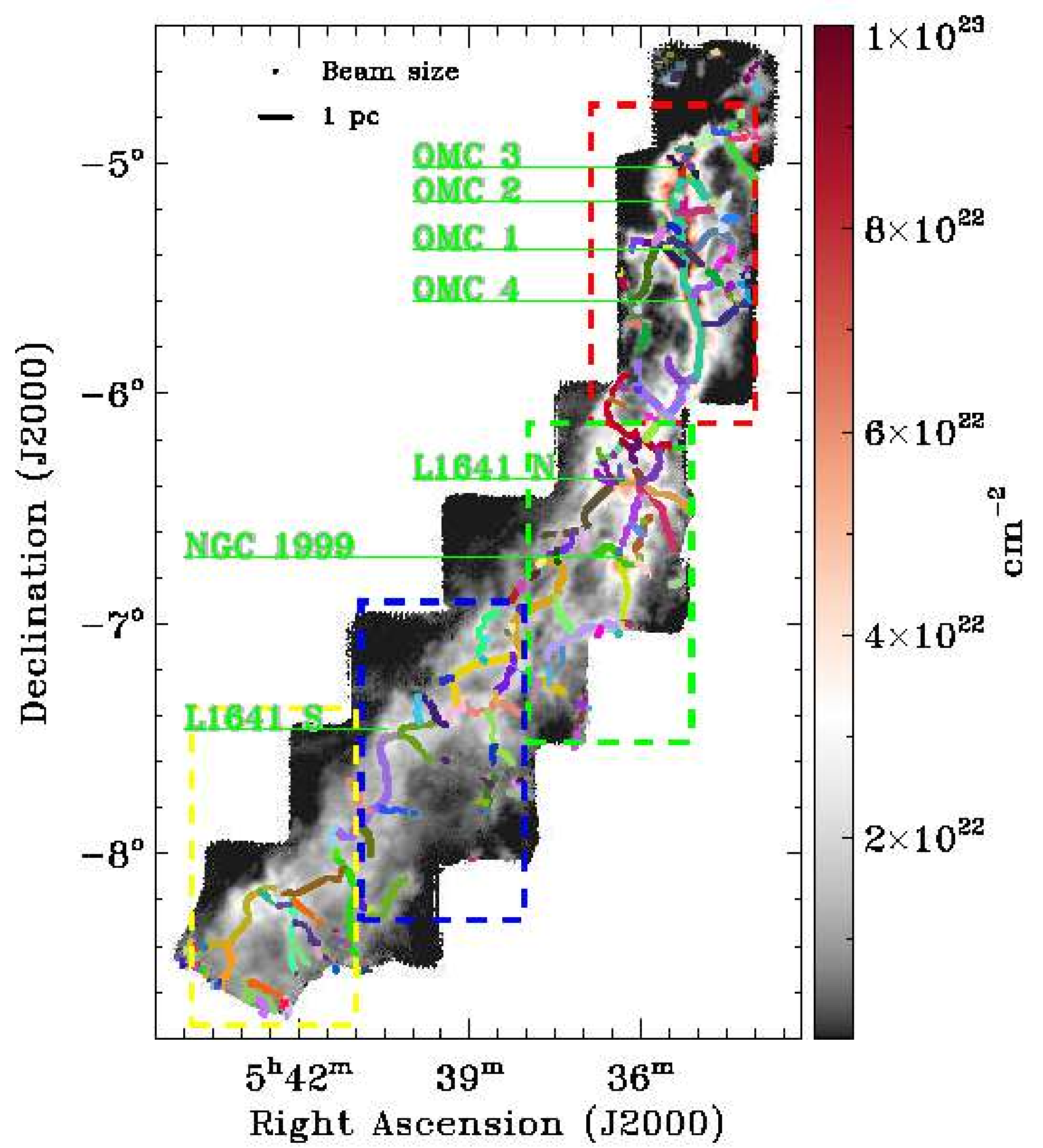

Zheng et al. (2021) identified 225 filaments

OMC-4

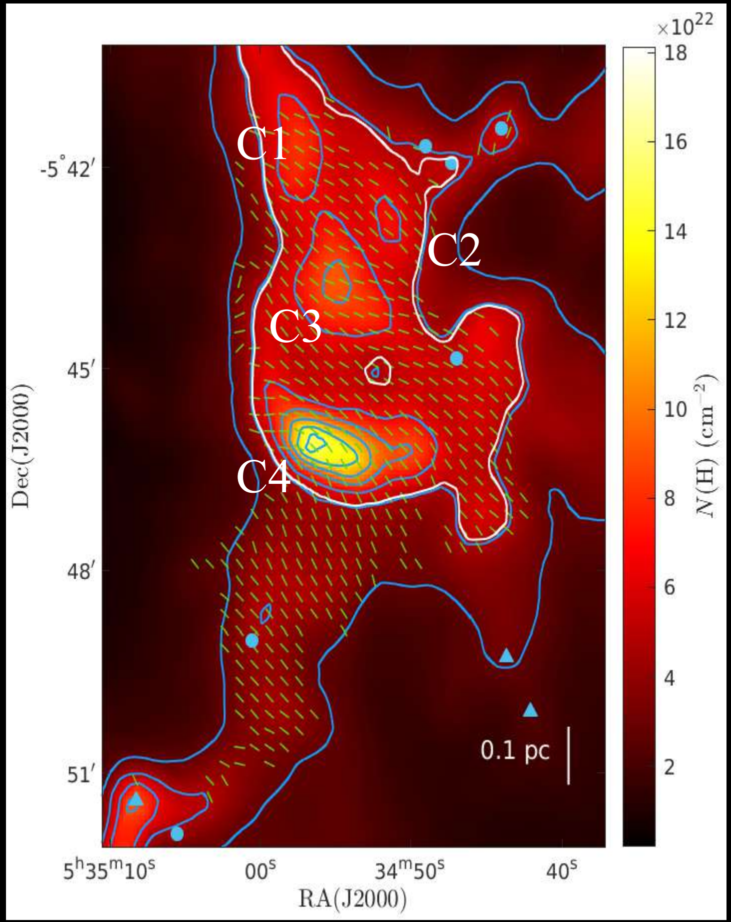

Simulation of the Formation of IRDCs

Large-scale magnetic field

Small-scale magnetic field

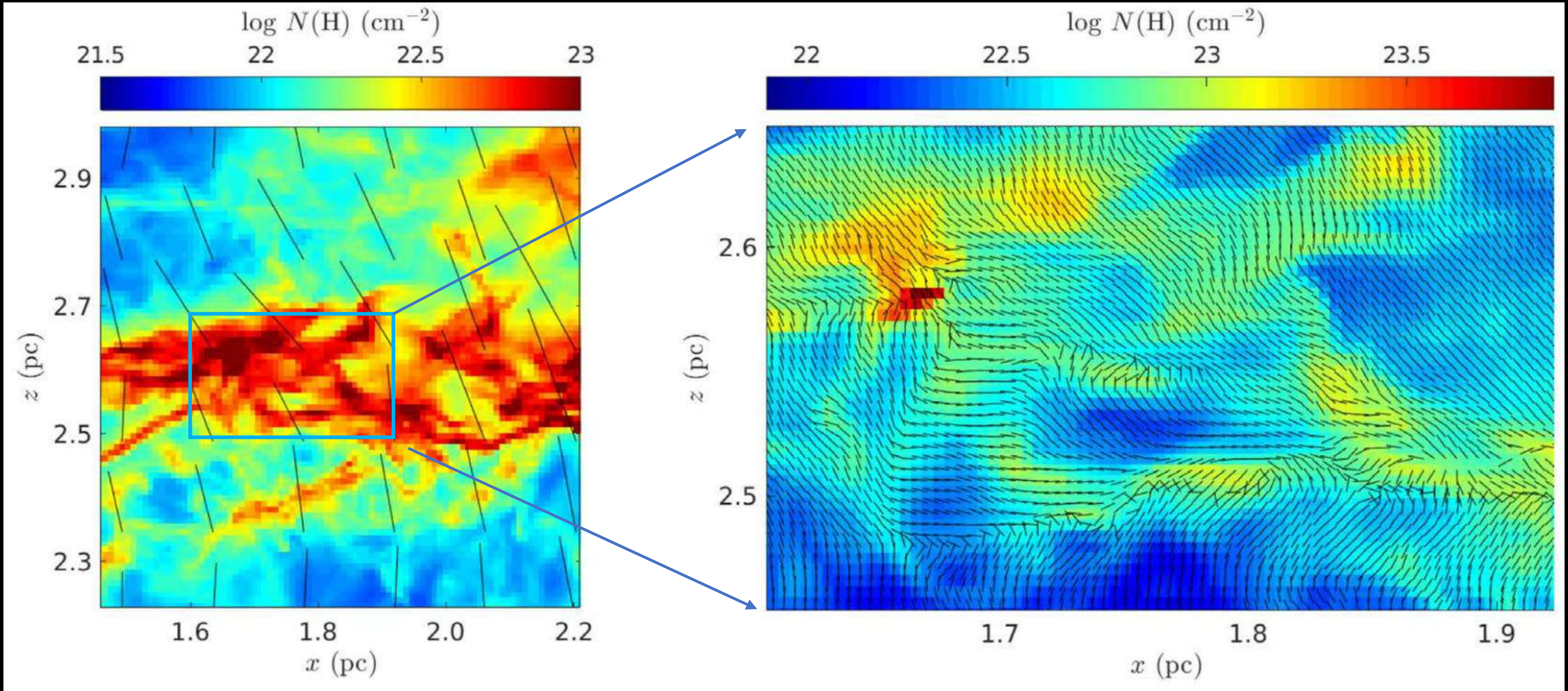

Li & Klein (2019)

Optical and Infrared Polarization Mapping of Taurus Region

Taurus Region

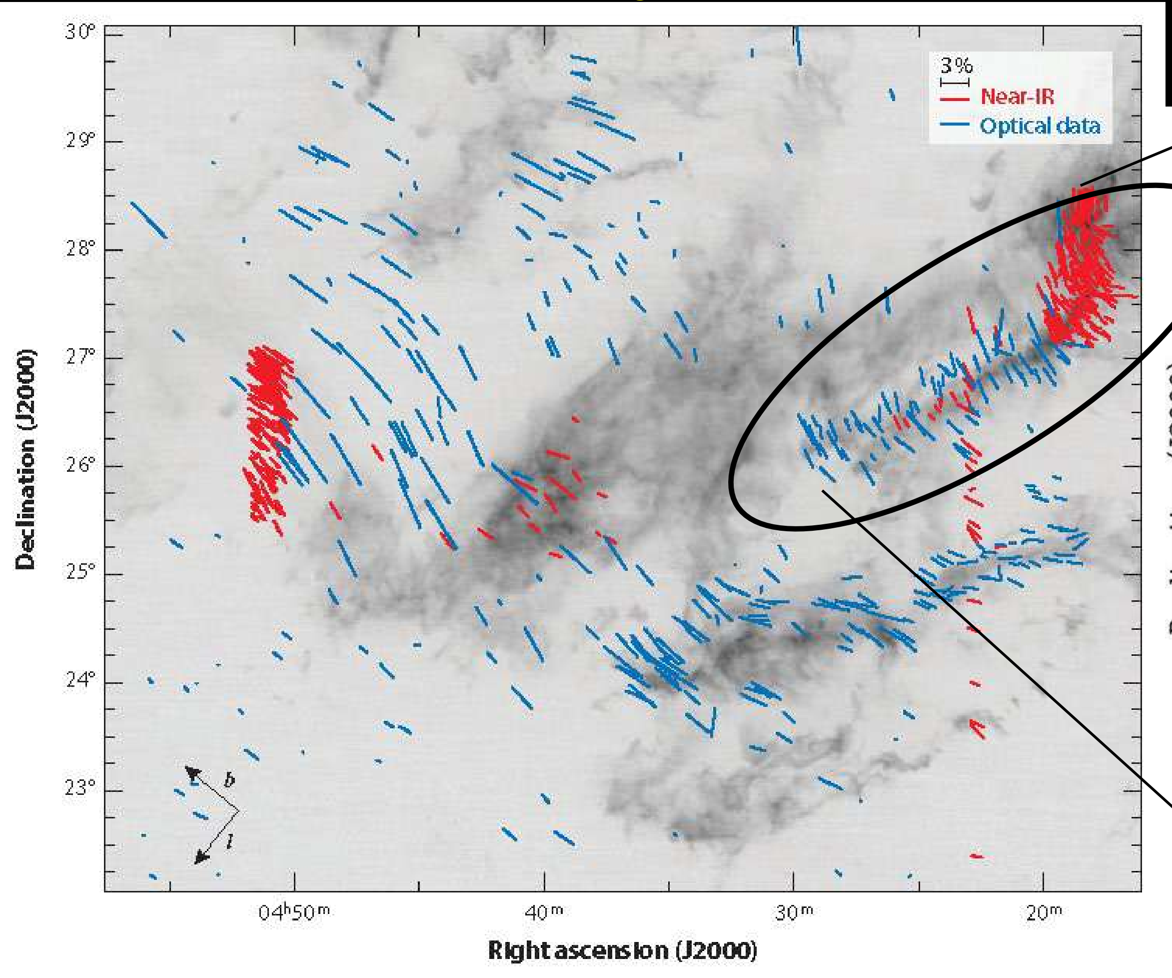

L1495/B7-218

Chapman et al. (2011)

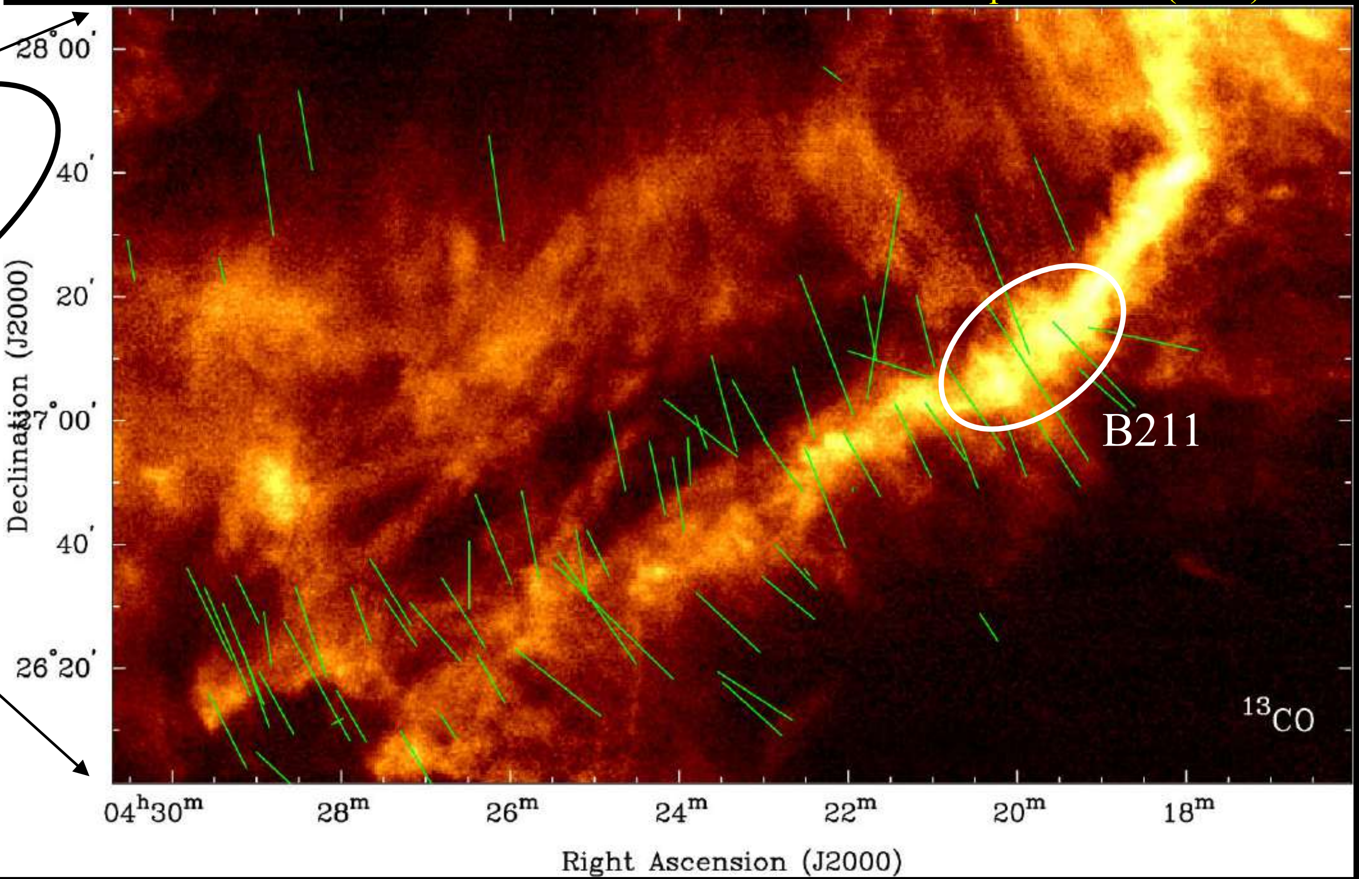

Inferred Magnetic Field Maps of L1495/B211 from Planck and SOFIA HAWC+

Large-scale magnetic field from Planck

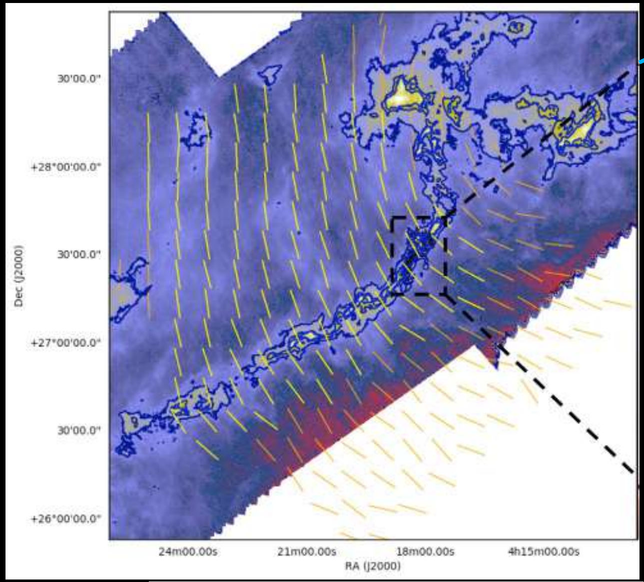

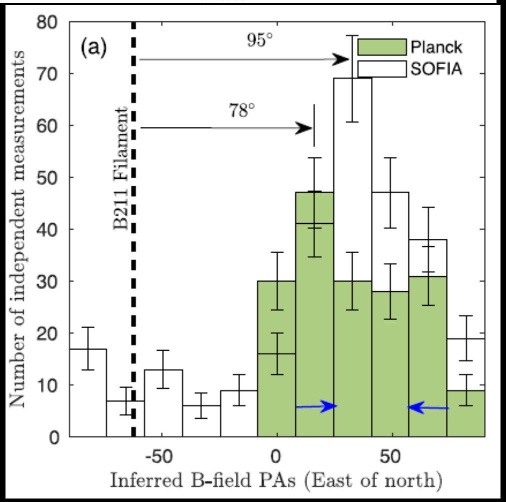

position angle distributions

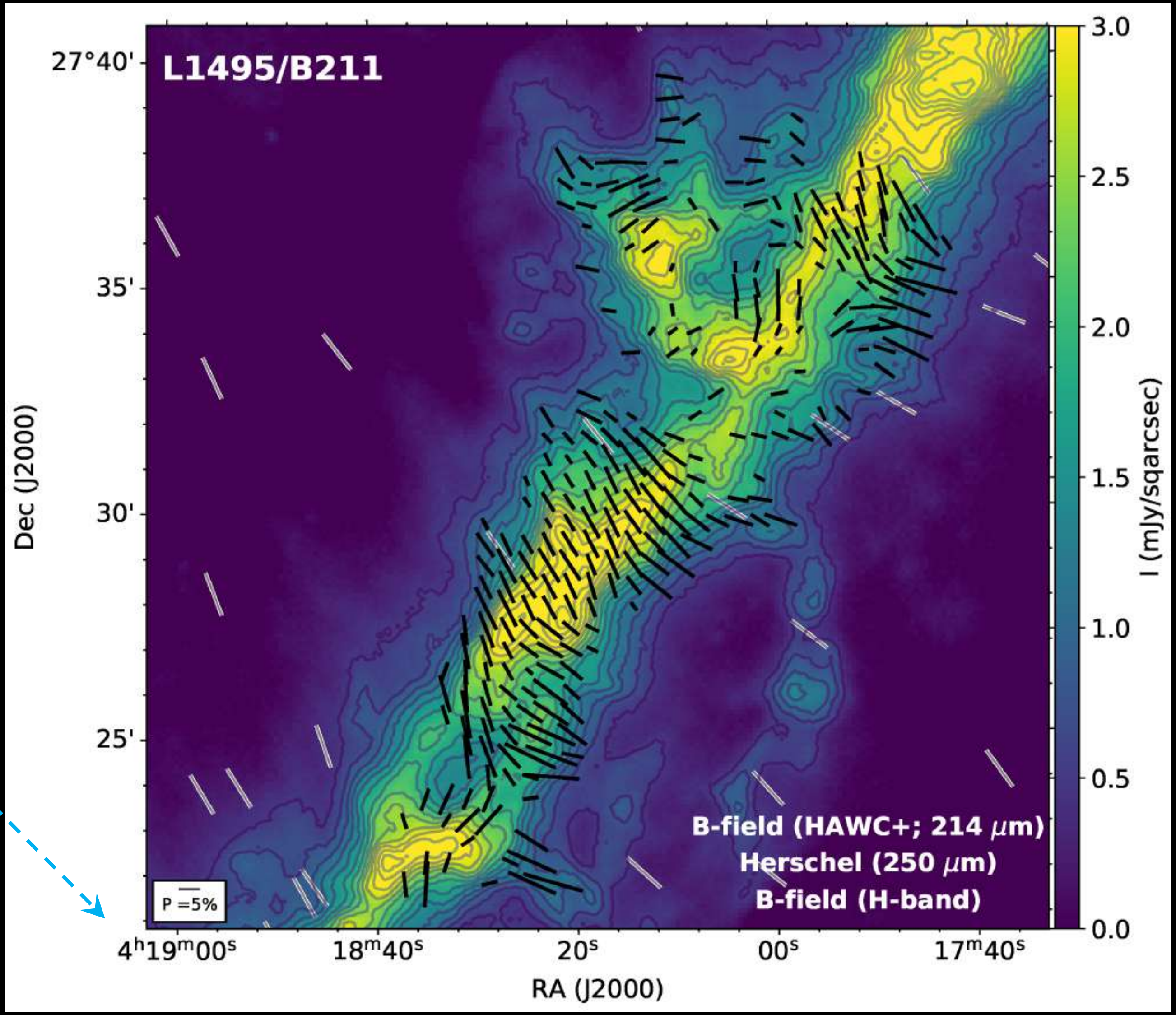

Li et al. (2022a)

Inferred Magnetic Field Maps of L1495/B211 from SOFIA HAWC+

Spurs: filamentary substructures merging with the main cloud
(e.g., Cox et a. 2016)

Hacar et al. (2013)

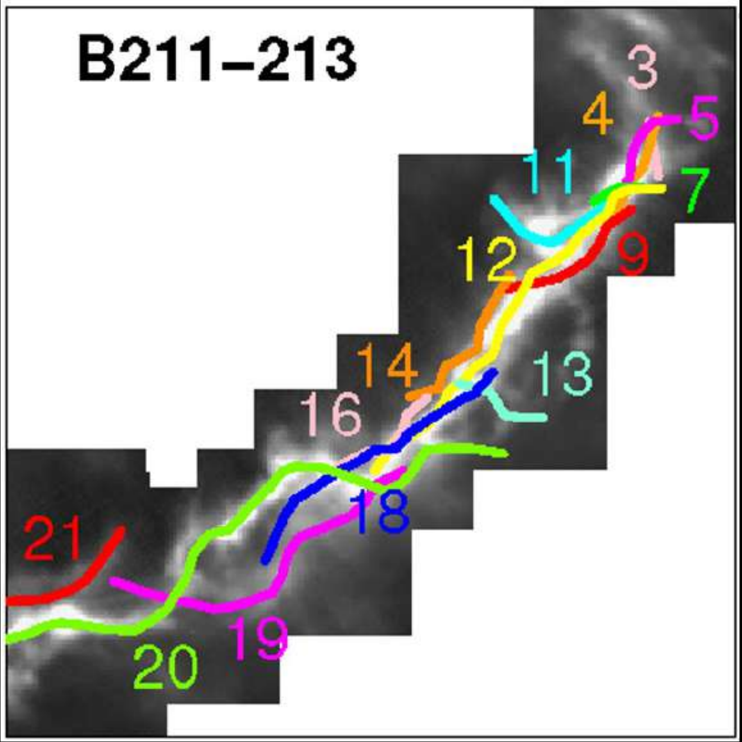

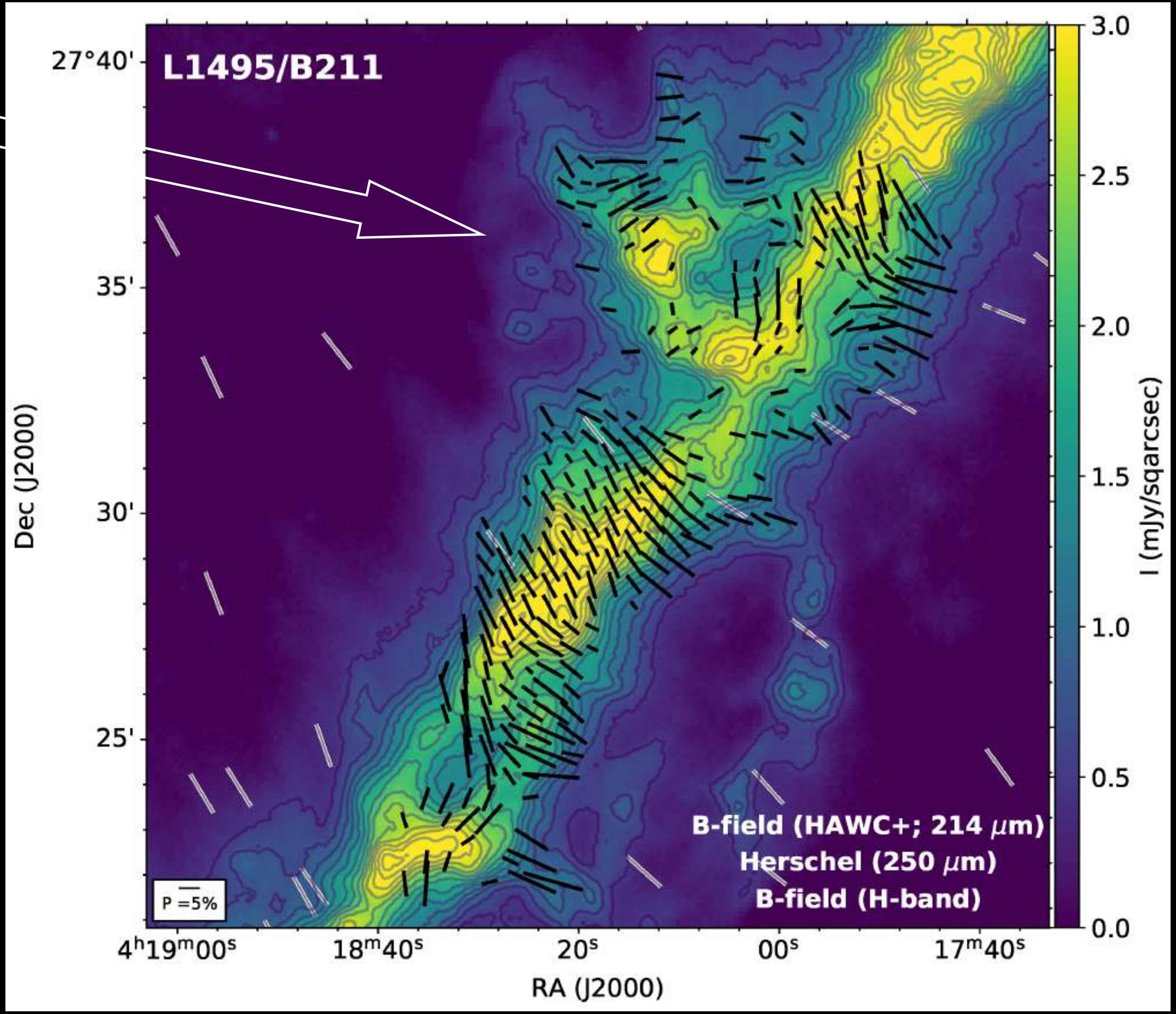

Li et al. (2022a)

Physical State of L1495/B211 from HAWC+, Herschel, and IRAM 30m Data

Li et al. (2022a)

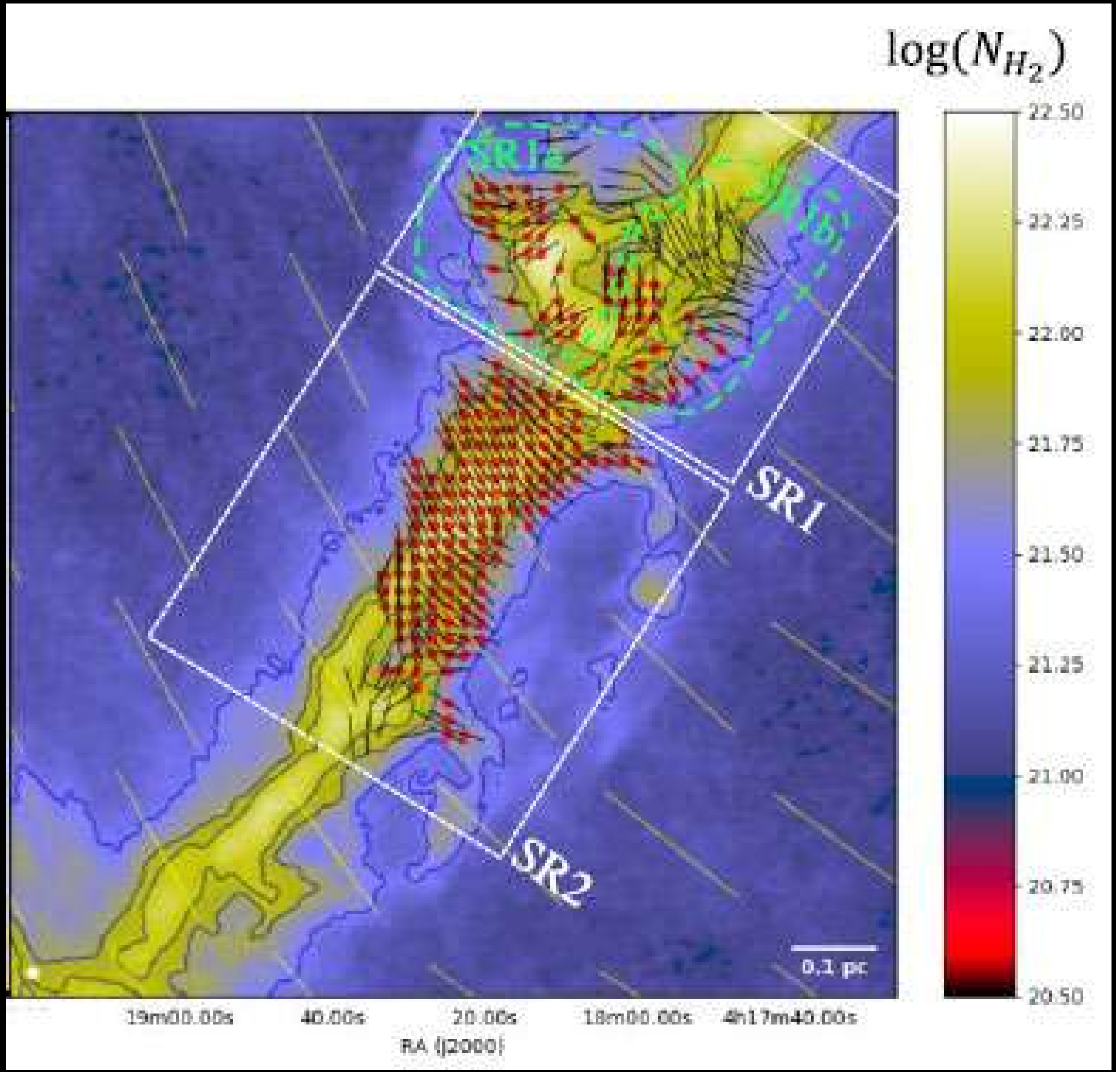

Region	SR1	SR2
M_ℓ ($M_\odot$ pc^{-1})	54	36
$\alpha_{\rm vir,f}$ [a]	2.0	2.2
$B_{0,\rm DCF}$ (μG)	13–23[b]	65–82
$B_{\rm tot,\,DCF}$ (μG)[c]	23–30	70–85
$\mu_{\Phi,\rm\,DCF}$ [d]	2.7–2.1	1.2–1.0
$\mathcal{M}_{\rm A}/\cos\gamma$ [e]	4.8–2.6	1.3–1.0
$M_\ell/M_{{\rm crit},\ell}$ [f]	0.50–0.49	0.43–0.42

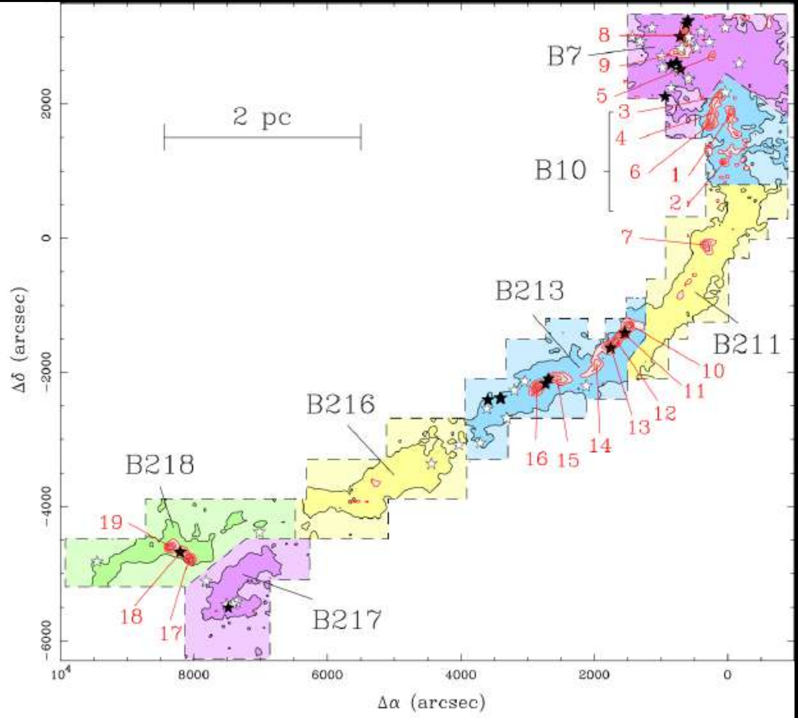

Hacar et al. (2013)

Conclusions

- Observed region of **OMC-3** by HAWC+ is **magnetically supercritical and strongly subvirial**. This region should be in the **gravitational collapse** phase and is consistent with many young stellar objects (YSOs) forming in the region.

- Observed region of **OMC-4** by HAWC+ is generally **magnetically subcritical except for an elongated dense clump**, which could be a result of projection effect of a filamentary structure aligned close to the line-of-sight. The dominating strong magnetic field in OMC-4 is **unfavorable for star formation** and is consistent with much fewer YSOs than in OMC-3.

- **Taurus/B211** is **super-virial and magnetically supercritcal**. The line-mass is smaller than the critical value and expected to be **gravitationally stable**. This is consistent with no YSOs found in the region.

- High resolution polarization map of **Taurus/B211** reveals large dispersion of magnetic field structure, a contrast to the highly uniform large-scale field structure around the cloud.

References:
Simulation: Li, P. S. & Klein, R. I. (2019)
Tarus/B211: Li, P. S., Lopez-Rodriguez E., Ajeddig, H., André, P., McKee, C. F., Rho, J., & Klein , R. I. (2022a)
OMC-3 & OMC-4: Li P. S., Lopez-Rodriguez E., Soam A., & Klein R. I. (2022b)